# DIRECTED ASSEMBLY OF CHARGED NANOPARTICLES BY USING ELECTROSTATIC FORCES IN A FLUIDIC MEDIUM

A THESIS SUBMITTED TO

THE GRADUATE SCHOOL OF ENGINEERING AND SCIENCE

OF BILKENT UNIVERSITY

IN PARTIAL FULFULLMENT OF THE REQUIREMENTS FOR

THE DEGREE OF

MASTER OF SCIENCE

IN

MATERIALS SCIENCE AND NANOTECHNOLOGY

By
Eliza Sopubekova
February 2019

DIRECTED ASSEMBLY OF CHARGED NANOPARTICLES BY USING ELECTROSTATIC FORCES IN A FLUIDIC MEDIUM

By Eliza Sopubekova

February 2019

We certify that we have read this thesis and that in our opinion it is fully adequate, in scope and in quality, as a thesis for the degree of Master of Science.

_____

E.Yegan Erdem (Advisor)

_____

Bilge Baytekin

_____

Batur Ercan

Approved for the Graduate School of Engineering and Science:

_____

Ezhan Karaşan
Director of the Graduate School

# ABSTRACT

# DIRECTED ASSEMBLY OF CHARGED NANOPARTICLES BY USING ELECTROSTATIC FORCES IN A FLUIDIC MEDIUM

Eliza Sopubekova

M.S in Materials Science and Nanotechnology

Advisor: E. Yegan Erdem

January, 2019

Deposition of nanoparticles in a controlled manner is suitable for the application of unique properties of nanoparticles in designing novel electronic devices. Printing different types of nanoparticles on the same surface generates multifunctional surfaces and opens up possibilities to elaborate future devices. Electrostatic forces can potentially be utilized to manipulate different types of materials such as magnetic, insulating, conducting, semiconducting, organic and inorganic materials. Moreover, chemistry of materials and the surface is not altered.

Herein, we applied these forces to direct and position charged nanoparticles on desired areas of the surface from nonpolar and aqueous dispersions. Assemblies of particles are obtained on both nonconductive surface with charged patterns and on metallic nano- and microstructured electrodes. Arrays of gold electrodes of sizes from 500 nm to 50 µm were prepared by using the conventional fabrication techniques such as photolithography, electron beam lithography, thermal evaporation and lift off. Charge patterns are formed on 100 nm PMMA surface which is coated on the electrodes to provide electrical contact. An external voltage was applied and substrate was immersed into desired aqueous negatively charged colloidal gold dispersion to direct nanoparticles on aforementioned charge patterns. The next step was to attract two different charged nanoparticles towards different locations on the same substrate by means of electrophoretic deposition. Assemblies formed from positively charged silver nanoparticles and negatively charged fluorescent latex and silica nanoparticles are demonstrated.

Last but not least, composite structures were obtained with similar techniques in order to increase the functionality of the structured surface. To achieve this goal, different types of nanoparticles were coated on top of each other without changing the location of electrodes. The shape of these composite structures is controlled by the electrode geometry.

*Keywords:* Nanoprinting, nanoimprinting, electrophoretic deposition, electron beam lithography

# ÖZET

# YÜKLÜ NANOPARÇACIKLARIN ELEKTROSTATİK KUVVETLER İLE AKIŞKAN ORTAMDA YÖNLENDİRİLMESİ

Eliza Sopubekova

Malzeme Bilimleri ve Nanoteknoloji, Yüksek Lisans

Advisor: E. Yegan Erdem

Ocak, 2019

Nanoparçacıkların kontrollü bir şekilde dağıtılabilmesi yeni ve özgün elektronik aygıtların dizaynının önünü açmaktadır. Aynı yüzey üstünde farklı panoparçacıkların istenilen şekilde yerleştirilmesi çok işlevli yüzeyler oluşturmaktadır ve bu yüzeyler yeni teknolojik uygulamaların önünü açabilir. Manyetik, yalıtkan, iletken, yarı iletken, organik ve inorganik gibi farklı özelliklerdeki parçacıklar Elektrostatik kuvvetlerin yardımı ile manipüle edilebilinmektedir. Bu yöntem aynı zamanda kullanılan parçacıkların ve yüzeyin kimyasına etkide bulunmamaktadır.

Bu çalışmada, bahsedilen etkiler kullanılarak apolar ve sulu dispersiyonlardaki yüklü parçacıkların yüzey üstünde köntrollü hareketi ve belirlenmiş alanlara toplanması sağlanmıştır. Bu ‘toplaşmalar’ yüklü yollar sayesinde yalıtkan yüzeyler üstünde ayrıca metalik mikro-nano boyuttaki elektrodlar üstünde elde edilebilmiştir. Boyutları 500 nm ve 50 μm arasında değişen altın elektrod demetleri fotolitografi, elektron ışınlı basım ve termal buharlaştırma gibi konvansiyonel teknikler kullanılarak üretilmiştir. 100 nm PMMA yüzeyi üstüne elektrik kontağı sağlaması amacıyla yüklü yollar basılmıştır. Bu yollara voltaj uygulanıp içinde eksi yüklü altın parçacıkların bulunduğu bir dispersiyona batırılarak parçacıkların yüklü yollar üstündeki kontrollü hareketi sağlanmıştır. Bir sonraki adım olarak iki farklı yüke sahip nanoarçacıkların elektroforetik bırakıntı kullanılarak aynı alt taş üstünde iki farklı bölgeye iletilmesi gösterilmiştir. Bu yöntem ile pozitif yüklü gümüş nanoparçacıkların ve negatif yüklü floresan latex ve silika nanoparçacıkların kontrollü toplaşması sağlanmıştır.

Yapılandırılmış yüzeyin işlevselliğini arttırma amacıyla, benzer bir teknik kullanılarak yüzey üstünde kompozit yapılar oluşturulmuştur. Bu kompozit yapılar elektrodların yeri değiştirilmeden farklı nanoparçacıkların yüzeyde üst üste ve yan yana biriktirilmesi ile yapılmıştır.

*Anahtar sözcükler*: nanobaskı, kontrollü nanoparçacık yerleştirme, elektroforetik kaplama, elektron ışın litografı

# Acknowledgements

First of all, I would like to express sincere gratitude and appreciation to my advisor Dr. Yegan Erdem. Her continuous support, encouragement and guidance have been motivated and inspired me throughout the time of my research and study. I would like to acknowlegde Dr. Bilge Baytekin and Dr. Batur Ercan Alpan for their time, helpful critics as the thesis committee.

I also thank Micro and Nano Integrated Fluids (MiNI) Research Group, both former and present members for the wonderful friendly environment during the the course of the years. Especially I thank Arsalan Nikdoost, Muhammad Saqib, Malik Abdul Wahab, Ecem Yelekli and Mayssam Naji for their help and support. I want acknowledge Dr. Güneş Kibar for her assistance with silver nanoparticle synthesis.

My deep gratitude also goes to the faculty and staff of UNAM and Mechanical Engineering Department for providing me a delightful atmosphere throughout my study.

I am grateful to my friends Khatidzhe Kandymova, Ulviyya Quliyeva, Assel Amirzhanova, Mehdi Ramezani, Mohammad Fathi Tovini, Koray Yavuz and Döölös Aybek uulu for always being next to me and for making my stay at Bilkent University bright and full of great memories.

Special thanks go to my beloved family: to my mother Gulmira Kozhakhmetova, to my father Nematilla Sopubekov, to my brother Mederbek Sopubekov, to my sister Elina Sopubekova, to my sister-in-law Ainagul Zholdosheva and to my nephew Manas Sopubekov for their endless support, love and care.

I acknowledge TÜBİTAK for providing the financial support for the project grant number 115M571.

# Contents

# List of figures

# List of Tables

# Chapter 1

# INTRODUCTION

Today, there have been remarkable advancements in fabrication, processing and applications of materials in nanometer size range. Nanoparticles attracted extensive attention due to their notable differences in physical, optical as well as electronic properties compared to bulk materials. These properties are dictated by particle's size and shape and they open up possibilities for nanoscale materials to be utilized in optical, electronic, sensing and biomedical applications. Moreover, the high surface to volume ratio of nanoparticles can be used to achieve highly porous materials with increased surface area and can be used for filtration and as catalysts.

Semiconductor nanoparticles know as quantum dots (QDs) have only few nanometers of radius and its size is on the same order as the exciton Bohr radius. Thus, by adjusting the size of a crystal, absorption and emission spectra can be controlled. Besides, the relatively sharp absorption and emission features incorporate wide spectral range from ultraviolet to infrared [1]. These aspects of QDs make them suitable candidates for various applications. Some of these applications are optoelectronic devices such as biological systems imaging [2], LEDs [3], solar cells [4, 5] and photodetectors [6]. Metallic nanoparticles gold (Au) and silver (Ag) are biocompatible and due to their particle-related photonic,

electronic and plasmonic characteristics, they can be used in biosensing [7], cancer diagnosis and treatment [8] and medical imaging [9]. Other types of materials such as magnetic and polymeric nanoparticles have also been studied for potential applications in biomedicine [10, 11]. Combination of different types of nanomaterials enhances the functionality and efficiency of the devices due to their collective features. For instance, energy sources such as solar cells, lithium-ion batteries and fuel cells can be manufactured by locating different types of semiconductor particles on the surface [12]. Furthermore, it's necessary to locate the particles on the surface in a controlled manner, since it's a crucial factor affecting the device's performance and functionality [13].

### 1.1 Review of Existing Methods for Nanoparticle Patterning

One of the main challenges in using the particles in an application is to be able to locate them in a desired pattern on an appropriate substrate surface. Various methods are established in order to print the nanoparticles on a surface. The most popular patterning method is photolithography which is also a top-down fabrication technique. Although it is widely used in both manufacturing industry and research, photolithography is adaptable for limited amounts of materials and has lack the resolution. This process is rather used to produce geometrical structures which assist in bottom-up patterning of nanomaterials. One of such bottom-up printing methods is called template assisted assembly. This method generally makes use of flexible polymer template in order to obtain the desired arrangement of nanoparticles on the surface. First, the structures on the template are prepared by optical or electron beam lithography followed by pouring the nanoparticle solution on to the mold. Next, this mold is pressed onto the desired substrate surface and finally the pattern is obtained. The process is also known as nanoimprint lithography [14]. It was observed that the molds prepared with electron beam patterning provide more precisely patterned nanoparticles with higher resolution [15]. The drawback of this method is that the residual layer, which must be etched away, is left on the substrate after the pattern transfer and it is limited for the patterning of only one type of nanoparticle on the surface.

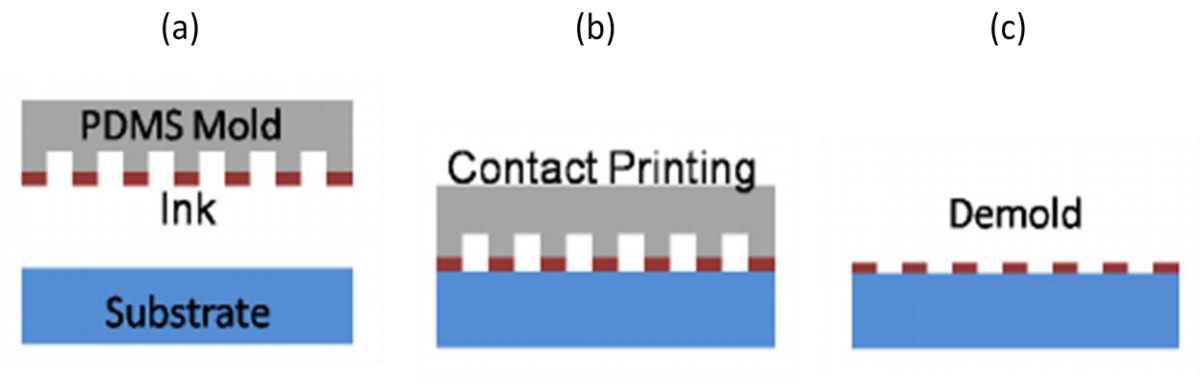


Figure 1.1. Nanoimprint Lithography steps (a) structured PDMS mold with target ink (nanoparticle) (b) pattern transfer onto substrate. (c) patterned substrate.

As a solution to the aforementioned problems, another method was proposed by Demko et al. [16]. They developed a microfluidic molding process where the patterns are obtained by the permeation pumping of the solvent containing nanoparticles. Namely, the solvent penetrates to the microchannels on the mold by capillary forces and it evaporates inside this permeable polymer mold by leaving the concentrated nanoparticles on the defined areas of the substrate. The formation of residual layer was prevented and versatile nanostructures could be obtained. However, this method is not applicable for the pattern geometries that are independent from each other and is finite for one type of nanoparticle assembly.

Another prominent process known for controlled placement of particles is inkjet printing [17, 18]. As its name indicates, the procedure is similar to the one that is used for conventional printers. The process of inkjet printing is shown in Figure 1.2 The particles that are suspended in a fluid are ejected to the surface through the nozzle to create a pattern. This method is popular for being simple and additive and the particle solution is not wasted because etching of the residual layer is not necessary. Nonetheless, the resolution of the printed pattern is around 20-50 μm [18], and the geometry control over the patterns is bounded. For obtaining finer features, methods with higher resolutions should be preferred.

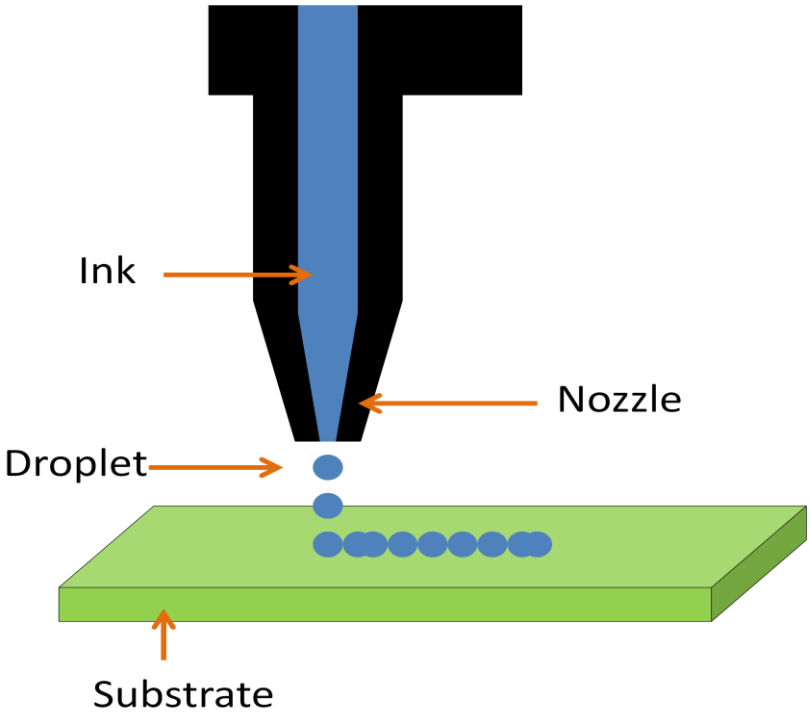


Figure 1.2. Inkjet printing method where the particles are ejected from the nozzle and form patterns.

For nanoparticle manipulation methods, it is essential to prevent from altering the surface to be patterned physically or chemically to provide flexibility in choosing the target material. The patterned surfaces with higher resolution can be produced when the chemistry of surface is not modified and when the microstructured physical barriers are removed.

Substitutions for the template-based methods are the ones that employ electrostatic forces to manipulate and direct the nanoparticles to form patterns. There are two approaches utilizing these forces. First approach is directing neutral nanoparticles in a fluid by means of dielectrophoretic forces in non-uniform electric field [19]. Second approach is to initiate the diffusion of charged nanoparticles towards the oppositely charged substrate surface as by using the Coulomb forces also known as eletrophoretic forces [20]. Both methods incorporate electrostatic attractive forces to direct and trap the particles on desired areas.

Wood et al. succeeded to locate the neutral gold nanoparticles on the nanoprobe surface by dielectrophoretic forces exerted as a result of non-uniform electric field between the nanoprobe and a metallic substrate [19]. Another method utilizing the electrostatic interactions is the one where the surface has electrically charged patterns and the particles possessing the opposite charge with respect to the surface is attracted towards the charged patterns [20, 21, 22, 23]. The first study demonstrating the utility of electrostatic forces for nanopatterning was done by Jacobs et al. in 2002 [20]. The thin layer of dielectric film on silicon substrate was polarized by conductive microstructured stamp and charged patterns were obtained. Next, the substrate was immersed into the nonpolar solution containing the charged iron oxide nanoparticles and the particles were trapped on the charge patterns as a result of electrical attraction. The same procedure was performed for carbon nanoparticles and the obtained result was the same. 1 μm wide patterns were created however they were not uniform due to the uneven distribution of charges on dielectric surface. Barry et al. [21] used the same method to produce iron oxide patterned surfaces. The stamp was made from PDMS coated with thin film of gold. The resolution was increased from 1μm to 100 nm which is remarkable. Kolibal et al. demonstrated an alternative way to obtain the charged patterns by applying ion beam to the dielectric surface; as a result, negatively charged gold nanoparticle patterns were created [23]. Although using ion beams is an innovative approach, modifying the surface with the charge is time consuming and it's not effective enough to uniformly deposit particles.

All the works mentioned above are significant in the field of nanopatterning. However, each of them has at least one of the drawbacks such as limitations on the material size and the geometry, time consumption, low resolution or the complexity of the method. Moreover, the obtained patterns consist of only one type of nanoparticle.

Over the last few years, the most versatile alternative for the controlled assembly of charged nanoparticles is believed to be atomic force microscope (AFM) nanoxerography [24, 25, 26, 27]. In this method, charge is written on the dielectric surface by applying the potential to the tip of the AFM cantilever and it allows

producing patterns of any kind of shape. Furthermore, Palleau et al. [26] proposed a two-stage development procedure to trap the particles directly from the aqueous dispersions. All the previous methods used particles either in nonpolar solutions or in solid and gas phases. Since the cantilever tip enables to write both positive and negative charges on the surface, it was possible to create the assemblies from two different types of particles (oppositely charged) [26,27].

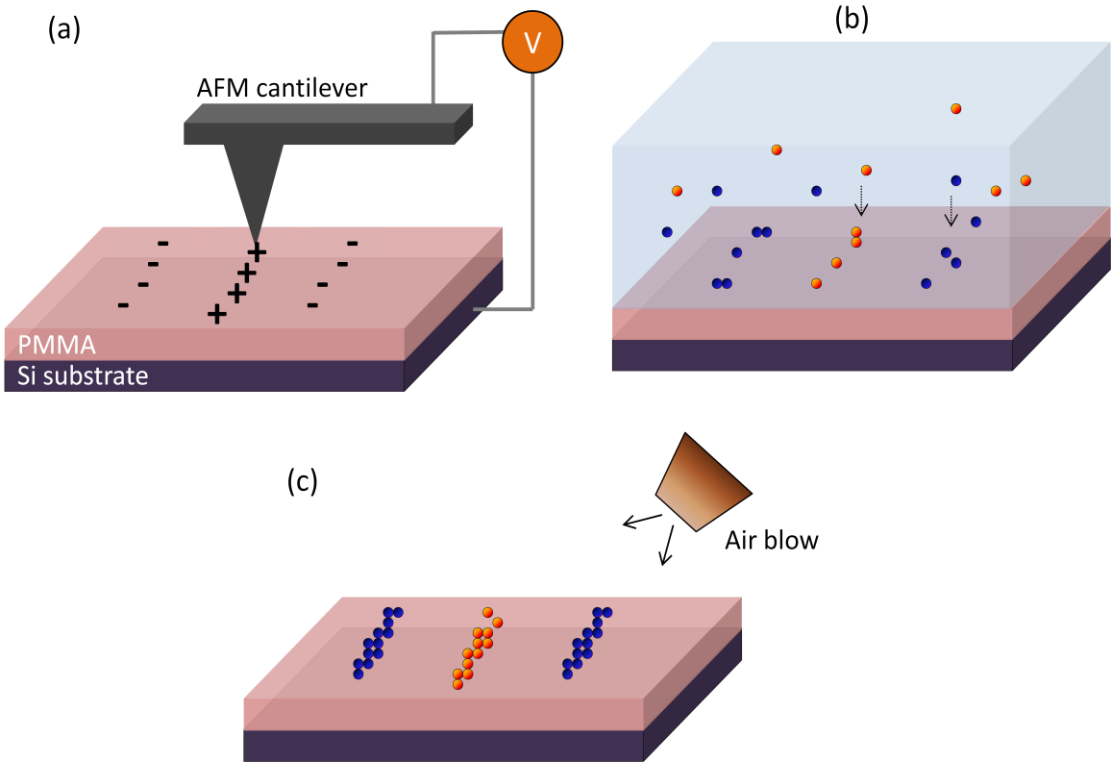


Figure 1.3. Schematics of AFM nanoxerography where the charged nanogels are electrostatically directed to the surface. (a) AFM charge writing on dielectric film (b) development in solvent after nanoparticles incubation (c) air blow drying.

AFM nanoxerography is the only method reported so far which allows to obtain patterns of two types of particles on the same surface. Yet, this approach requires high voltage (~80 V) to polarize the surface, single scan image size is 150µm×150µm which makes it complex and time consuming to pattern particles on larger surface areas.

In the research work presented here, directed assembly of various charged nanoparticles on polarized dielectric surfaces as well as on metallic structured surfaces by using electrostatic forces was demonstrated. The method that is used

here is applicable for all types of nanoparticles having surface charge and it is possible to pattern them on the same surface next or on top of each other thus making composite structures. Existence of two or more types of nanoparticles on the same surface is beneficial to combine their unique properties in multifunctional smart surfaces. For example, by placing the gold particles on one location and iron oxide particles on the other location of the same surface, it will be possible to design a nanosensor with two sensing qualities. Composite nanostructures consisting of nanomaterials carrying photonic, electronic, biological and chemical properties are critical to produce sensors with increased functionality and efficiency [28]. There exist a few work in literature on composite nanostructures. Yu et al. [29] used spin coating technique to obtain nanocomposites made up of gold and titanium dioxide nanoparticles. Each of the particles was coated one after another forming two layers of thin films. However, these composite structures are continuous on the surface and the shape cannot be controlled due to the nonselectivity of applied coating method. Electrostatic forces were also used to coat the particles on top of each other [30]. Layer by layer technique was used where the substrate surface was modified with electrical charge and one by one was immersed in to solutions containing nanoparticles with opposite polarities. Layers of different types of materials were obtained and it was used for biomedical applications.

Herein we show that the shape of the composites can be controlled by the shape of the electrodes onto which the particles are directed.

## 1.2 Electrostatic Interactions in Colloidal Solution

Stability of the colloidal nanoparticle solution is a key parameter for their precise and controlled deposition on the substrate. The particles should have a net surface charge so that the repulsive forces between particles will dominate and form the stable solution.

The aqueous media can consist of ions, polyelectrolytes or surfactants. When the particle is dispersed into this solution, free ions form an ionic cloud and the particle acquires electric surface charge as a result of electrostatic interactions.

The thickness of an ionic cloud is known as Debye length $1/K$ where $K$ is the Debye-Huckel parameter. [31]The charged nanoparticles have potential φ which is given as follows [32]:

$$\varphi = \frac{\sigma}{K\varepsilon} e^{-xK} \quad (1)$$

where $x$ is the distance from the surface of the particle, σ is the surface charge density and ε is the dielectric constant. Debye length can also be defined as the maximum distance affected from electrical force of the particle and it can be calculated by the following formula [32]:

$$K^{-1} = \sqrt{\frac{\varepsilon KT}{2nq^2}} \quad (2)$$

where $K$ is the Boltzmann's constant, $T$ is the temperature in Kelvin, $n$ is the particle density around the surface, and $q$ is the electrical charge. The distribution of the ions in the ionic cloud has a diffusive structure because of the thermal motion of the ions and the ionic cloud combined with the surface charge forms and electrical double layer (EDL), also known as diffuse double layer. The EDL potential exponentially decays with the Debye lenght as it is shown in Figure 1.4

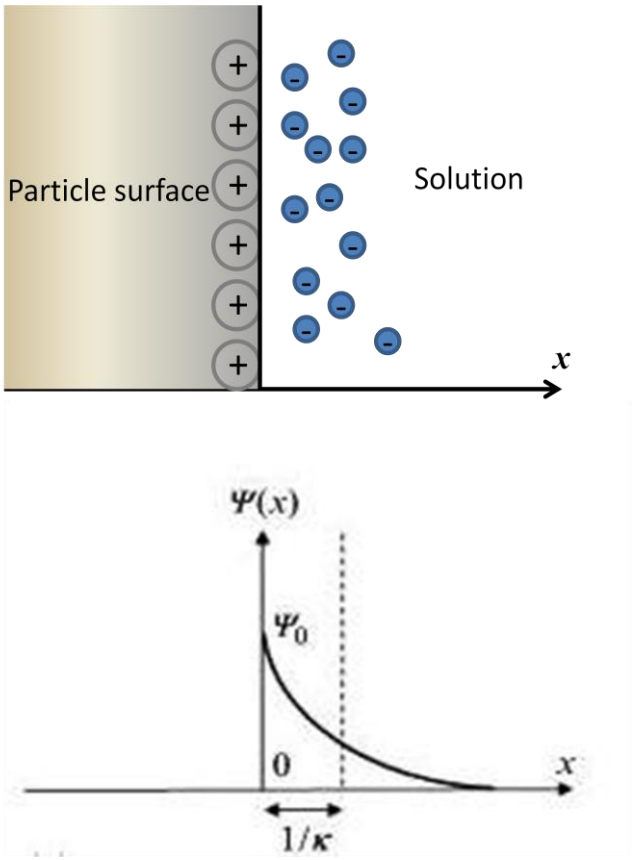


Figure 1.4. Representation electrical double layer (EDL) on the top and electrical potential decay on the bottom .

Another phenomenon that keeps the particles stable in the fluid is known as Brownian motion [33]. Brownian motion is the random movement of particles in a solution due to their collisions with the molecules of the solvent. A macroscopic example is the diffusion where the particles move from higher concentration to lower one. The factors that affect the rate of this transport phenomenon are the temperature of the medium, number of particles, amount of solvent ions and the viscosity of the solvent.

### 1.3 Diffusion of Nanoparticles Driven by the Electrostatic Forces

As it was mentioned in section 1.1, the nanoparticles are directed towards the desired areas by electrostatic attraction forces. For example, the charge is written on the surface of thin dielectric film followed by exposing the substrate to the nanoparticle suspension. The polarization mechanism is shown in Figure 1.5

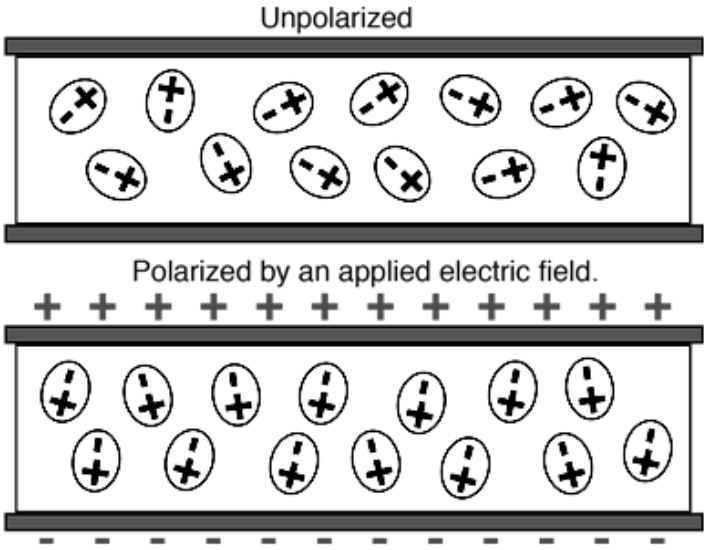


Figure 1.5. Unpolarized vs. Polarized dielectric material.

When there is no electric field, the polar molecules in dielectric material (such as PMMA) are in random position. An applied electric field polarized the material where the dipole moments of the polar molecules orient according to the field direction. Thus, internal electric field in dielectric layer is generate and it's in the opposite direction with respect to the external applied field. And when this external field is detached, the surface remains polarized. The studies showed that PMMA can retain charge without its planar diffusion up to 24 h [34]. After obtaining the charged surface, it is immersed into the oppositely charged solution to attract and assemble the particles.

### 1.3.1 Electrophoretic Deposition

Electrodeposition is a well known surface modification method that is used to create in situ coatings by applying an electric field. An electrolyte is a salt solution which contains the metal ions that will be targeted from counter electrode (anode) towards the working electrode (cathode) and reduction reaction occurs which results in the formation of target metal on the surface. On the other hand, electrolyte is charged nanoparticle suspension in electrophoretic deposition (EPD). Thus, no chemical reaction occurs on the electrode surfaces which make this technique more practical and versatile over electrodeposition. The first study that utilized the electrophoresis concept goes back to $19^{th}$ century where the electrode was coated with clay materials in the water [35]. The experimental setup

is very simple, it consists of working and counter electrode (anode and cathode depending on the direction of electric field and surface potential of nanoparticles) and charged nanoparticle solution. Several factors that affect the deposition rate are the followings:

- Conductivity of the substrate
- Applied voltage
- Distance between the two electrodes
- Surface area of the electrodes
- Concentration of the nanoparticle solution
- ζ-potential of the suspension
- Particle size
- Dielectric constant and viscosity of the solution
- Deposition time

EPD is most commonly used to produce thin films of nanoparticles adsorbed on the continuous metallic surface [36, 37, 38]. Only few studies on shape controlled coatings were reported. One of them was proposed by Majetich et al [39] where they located the iron oxide nanoparticles to the desired areas by putting the geometric barriers made of hydrogen silsesquioxane (HSQ) on the electrode surface.

It is worth pointing out that EPD is preferable for nonpolar solvents when DC voltage is applied. When it comes to aqueous solutions, there occurs electrolysis of water across the electrode due to the ion transfer and bubble generation interrupts the nanoparticle diffusion. Usage of organic solvents has drawbacks such as higher cost, low dielectric constant which requires higher voltage for deposition. Some nanomaterials are unstable in organic solvents and hence the conventional EPD technique cannot be applied.

As a solution to this problem, Uchikoshi et al. proposed employing pulsed DC voltage instead of continuous DC voltage to suppress the bubble formation [40]. Their results indicate that when pulse width lower than 1ms was applied at 50% duty cycle, there was not or very little amount of gas evolution on the electrodes. The reason is that the electrolysis was significantly decreased by shocking the reaction system with constantly pulsing current voltage. Namely, $H_2$ is produced from proton reduction and $O_2$ is produced from hydroxyl in water electrolysis [41]. Reaction rate is slow due to the transfer of more than one electron. The frequency of the pulsed voltage is high enough to slow down this reaction.

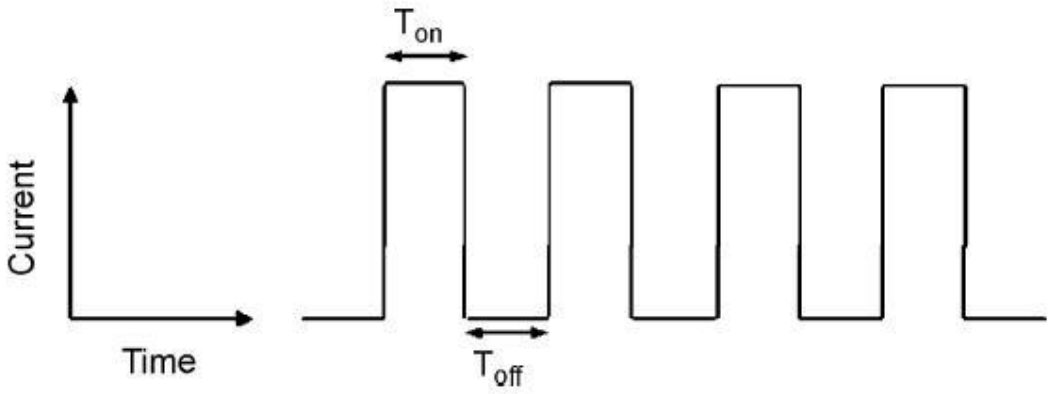


Figure 1.6 Schematic of pulsed current at 50 % duty cycle.

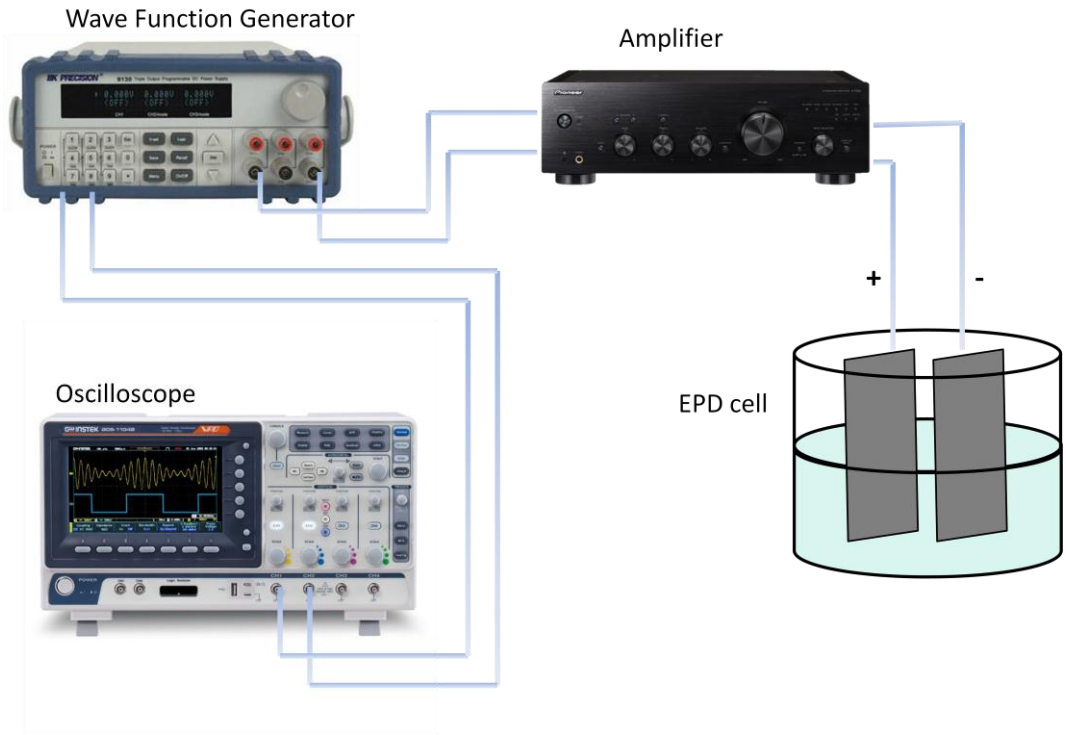


Figure 1.7. Experimental set-up for pulsed voltage electrophoretic deposition.

Instead of DC power supply, signal generator, amplifier and oscilloscope is used to generate the pulses of voltage. High frequency generator produces pulsed signal and its width, frequency and amplitude can be arranged according to the experimental requirements. The amplified signal is monitored in oscilloscope.

### 1.4 Thesis Organization

This thesis describes a directed assembly of charged nanoparticles by utilizing electrostatic forces. The patterned surfaces consist of one type of particles, two types particles on different locations and composites of two types od particles on the same areas.

Chapter 1 includes an overview on existing nanopatterning methods, theory behind the electrostatic interactions and nanoparticle diffusion and motivation behind the project.

Chapter 2 provide information about materials and methodology is given together with experimental details

Chapter 3 demonstrates the experimental results and their detailed discussion.

Chapter 4 gives a brief conclusion of this thesis with future outlook.

# Chapter 2

# MATERIALS AND METHODS

## 2.1 Fabrication of Electrodes

The design of electrodes plays an important role in guided assembly of the nanoparticles onto the desired areas of the surface. The parameters that directly affect the resolution and quality of the printed patterns are geometry and dimensions of the electrode and substrate surface on which it is located. For instance, the smaller the dimensions of the electrode, the higher the resolution of the achieved nanoparicle patterns. Consequently, electrodes were prepared by using cleanroom facilities in National Nanotechnology Research Center (UNAM). Both photolithography and electron beam lithography were employed for the fabrication

### 2.1.1 Mask Design and Fabrication

Electrodes that were fabricated from photolithographic techniques were designed in layout editor software tool L-Edit. This design was written on the glass substrate with chrome film in cleanroom. The top view of the mask design is shown in Figure 2.1. The electrode dimensions are listed in Table 2.1. These masks were produces in METU MEMS facilities.

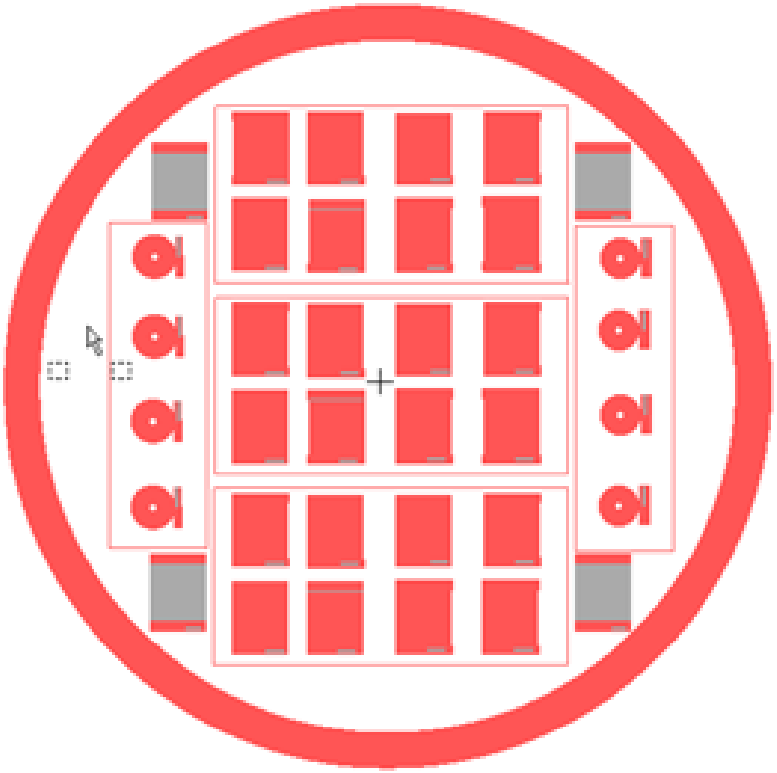

Figure 2. 1. L-Edit mask of the electrodes for fabrication in photolithography

Table 2. 1. Electrode dimensions on the mask.

| Design # | Rectangular shape | | Tori-like shape | |
|---|---|---|---|---|
| 1 | Width (µm) | Gap (µm) | Width (µm) | Gap (µm) |
| 2 | 20 | 40 | 20 | 20 |
| 3 | 20 | 20 | 20 | 40 |
| 4 | 30 | 50 | 20 | 60 |
| 5 | 10 | 10 | | |

In order to be able to apply both positive and negative voltages to the electrode surface, comb-like shapes were designed. Figure 2.2. shows the closer view of the electrodes.


Figure 2.2. Comb-like electrode design for both positive and negative charging.

Some of the electrodes are designed for applying only one type of voltage. Closer view is displayed in Figure 2.3.


Figure 2.3. Electrode design for positive or negative charging

Closer view of tori-like shaped electrodes are given in Figure 2.4. These electrodes can be charged with either positive or negative voltage.

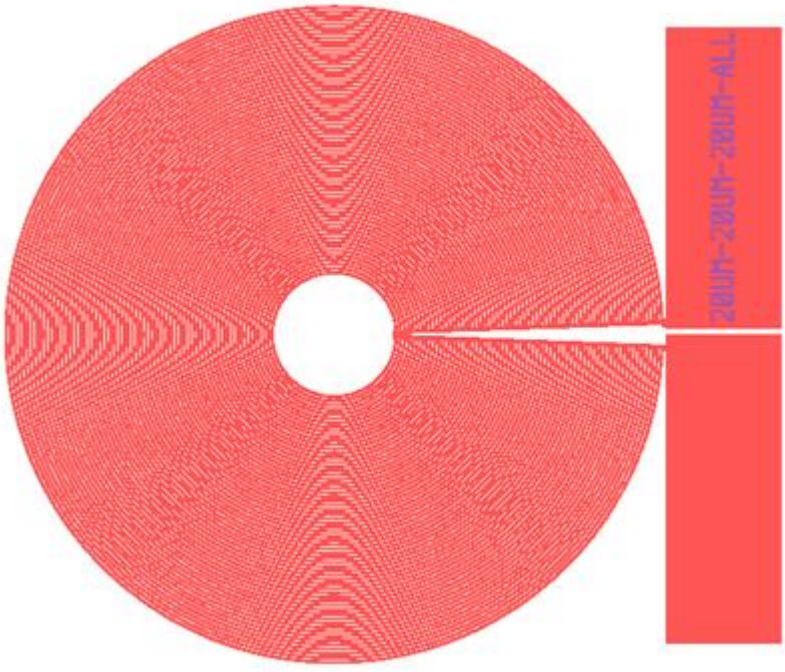


Figure 2.4. Tori-like electrode design for positive or negative charging.

### 2.1.2 Electrode Fabrication with Photolithography

First, 4 inch silicon wafer substrate coated with 90 nm thick silicon dioxide ($SiO_2$) was washed with acetone, isopropanol and DI water and dried with $N_2$ prior to use. Thin layer of gold was deposited to the substrate by employing thermal evaporation technique. Thermal evaporation is the subset of physical vapor deposition which provides uniform smooth layer of material on the substrate. Precursor is loaded to the conductive boat and is melted by applying DC electrical voltage to the boat. These boats should withstand high temperature and high current (~100 A) and there should not be any chemical reaction with the precursor. Commercially available tungsten oats were used for our fabrication. Evaporation of metal is done in ultra high vacuum chamber ($\leq 10^{-6}$Pa) in order to minimize the interaction of evaporated atoms with air molecules. In order to increase the adhesion between gold and $SiO_2$, the substrate surface was coated 5 nm of chromium and then 100 nm of gold was deposited. The adhesive Cr layer assures proper wet-etching and lift-off.

Next, the desired shape to the electrodes were given by photolithography. Positive AZ 1505 was used as photoresist (PR). This is the type of photoresist in which UV light exposed portions become soluble to the photoresist developer whereas unexposed areas remain insoluble in the developer. AZ 1505 serves as sufficiently stable mask and compatible with gold etching. PR was spin-coated at 3000 rpm for 40 s on the substrate (containing gold layer) and 580 nm of resist film was obtained. Then substrate was prebaked for 90 s in 110 °C oven and was exposed to UV light with exposure dose 20 mJ/cm$^2$ and by using the photomask described in section 2.1.1. This photomask protects the areas of electrode geometries from the UV exposure. The substrate was then postbaked for 50 s at 115 °C and developed in AZ 400K developer diluted with water (1:5 ratio) for 1 min and the desired pattern was obtained.

Before starting the etching process, the wafer was cut into small pieces with the dicing saw so that electrodes were separated from each other. Making these chips with separate electrodes helped to optimize the etching rate of gold. The most suitable etchant for gold is Aqua Regia. Its components are nitric acid and

hydrochloric acid in the ratio of 1:3 and it has slightly yellow color. Etching rate of Aqua Regia is 10-15µm/min. It is very high rate for 100 nm of gold therefore the etchant was diluted with 10 parts of DI water to get more precise pattern and to avoid undercuts. It took 50 s to etch the gold which means the etching rate of this diluted Aqua Regia 83 nm/min. Then the chip was washed with plenty amount of DI water to get rid of any traces of acid. The next step was to etch the adhesion layer underneath gold which is 4 nm of chromium in our case. It was etched in chromium etchant CR01 which is a mixture of perchloric acid and ammonium nitrate. 5 nm was etched in 10 s which makes its etching rate 24 nm/min.

At last, the electrode chips were immersed into AZ100K remover to dissolve the residues of PR that was exposed to UV light. Figure 2.5. Demonstrates the schematics of the fabrication steps.

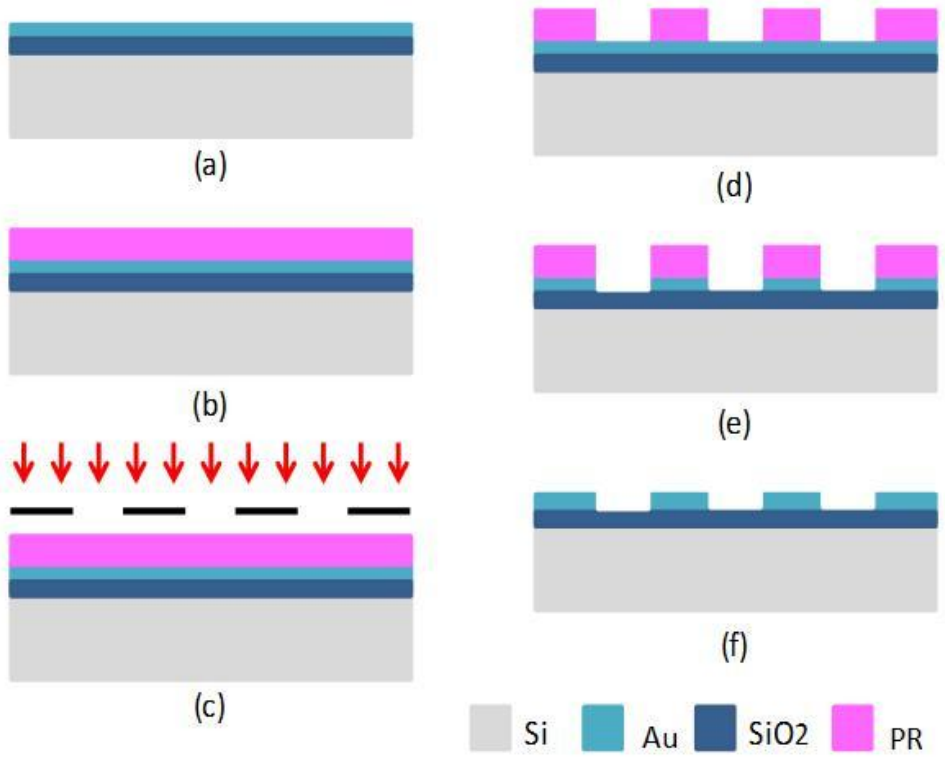


Figure 2.5. Schematics of fabrication steps of electrodes obtained with photolithography. (a) Thermal evaporation of 100 nm gold film on $SiO_2$ substrate. (b) Photoresist spin-coating (c) Transferring electrode patterns to PR surface by using UV exposure (red arrows) and photomask (black lines). (d) PR development

(e) Wet etching of metal (Au and Cr). (f) Removing PR residues from electrode surface.

As it was stated in Table 1 , fabricated rectangular electrodes have width varying from 10 µm to 30 µm and length is 8mm. Tori-like electrodes have 20 µm width and 3mm radius. SEM images of both electrode geometries are shown in Figure 2.6.

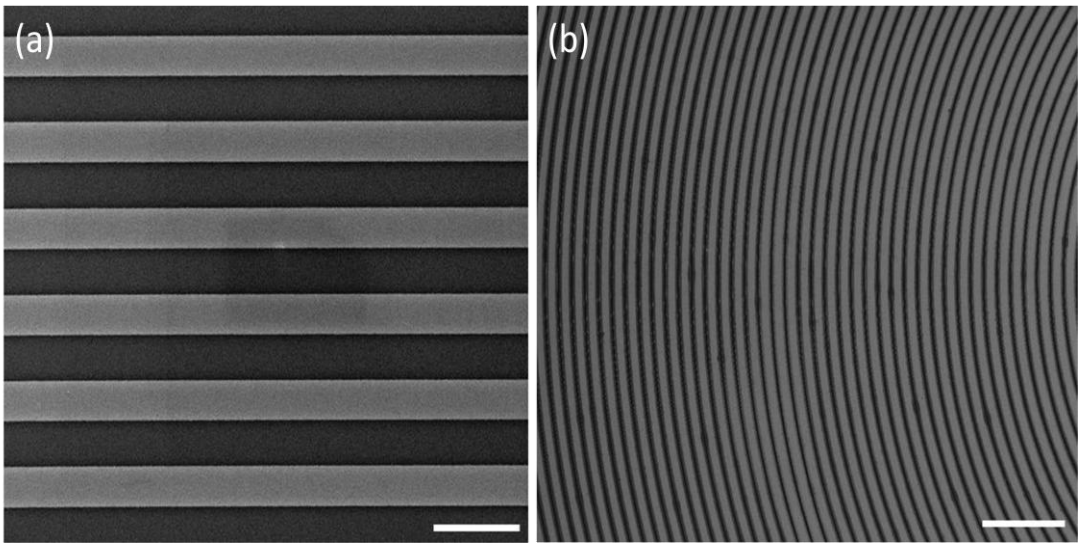


Figure 2.6. SEM micrographs of gold electrodes. a) Rectangular shape (electrode lines are parallel to each other) b) Tori-like shape. Scale bars are 50 and 250 µm for (a) and (b) respectively.

### 2.1.3 Electrode Fabrication with Electron Beam Lithography

Despite the fact that optical lithorgraphy is precise, efficient and cost-effective technique, it has limitations to project smaller nanostructured features onto the substrate due to the light (UV) that is used. More effective way to produce features at nanoscale is using electron beam lithography (EBL). As its name indicates, EBL uses electron beams to write patterns on the photoresist and it is not limited by the diffraction of incident light. By adjusting parameters such as sample preparation, design features, dose and speed of the exposed beam, one can obtain sub 100 nm size nanostructures. We utilized EBL to fabricate electrodes having feature sizes less than 1 µm. The whole setup consists of SEM (FEI-Nova

NanoSEM-600) and Raith pattern generator. Design of electrodes is drawn in software program ELPHY.

The substrate surface should be clean and free from any contamination prior to exposure. First, 4 inch silicon wafer having 90nm $SiO_2$ is cut into 15 $cm^2$ pieces and each of them was washed with acetone, isopropanol, and DI water respectively. It is followed by the drying of the sample in 120 °C oven for 10 mins. Polymethyl methacrylate (PMMA) serves as photoresist since it is sensitive to electron beam and is convenient for fine feature patterns. 100 nm of PMMA 495K A2 was spin-coated on the substrate surface followed by spinning PMMA 950K A4. 495K and 950K refer to the molecular weight of PMMA (i.e PMMA has 485 *kDa* and 950 *kDa* chain lengths respectively). A refers to the solvent anisole which is more environmentally friendly than chlorobenzene and 2 (and 4 for 950K PMMA) means that the solvent contains 2wt% of PMMA. The bilayer photoresist is used to increase the precisionof the features. More specifically, PMMA 495K has shorter polymer chains which makes the bottom layer more sensitive to exposed beam in contrast to 950K one. It should be noted that the sample was baked at 180 °C for 10 mins after each spin coating to remove the remaining solvent residues. Then comes the lithography step and the specimen was developed in methyl isobutyl ketone and isopropanol mixture (MIBK:IPA 1:3) for 50 s, then agitated in IPA for 20 s, rinsed in DI water and dried under nitrogen gas blow. After completing the lithography and development are complete, the sample is coated with 5nm of chromium and 100 nm of gold by thermal evaporation (the process is described in section 2.1.2. The completing step of the fabrication is to get rid of undesired metal layers by lift-off. The sample was left in acetone bath overnight to dissolve the unexposed portions of PMMA and hence to strip away the metal layer on top. Thus, fabrication of the EBL electrodes was complete and the comb electrode with 500nm width is shown in Figure 2.7.

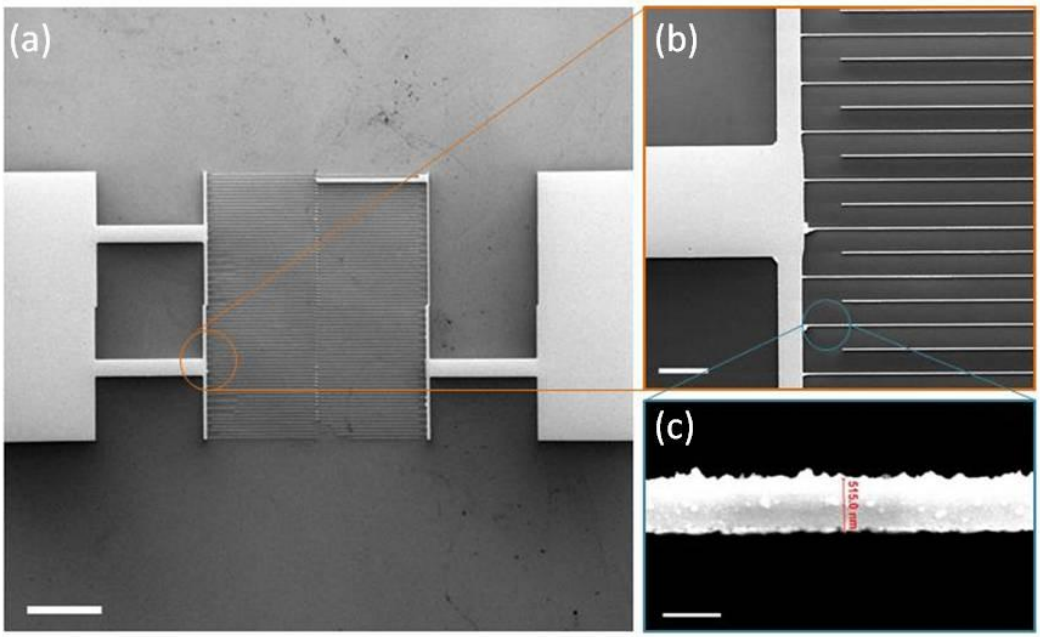


Figure 2.7. SEM images if 500nm comb-like electrode lines fabricated from EBL. Scale bars are 250, 25 and 0.5 μm for (a), (b) and (c) respectively.

Since the writefield area in EBL was 400 $\mu m^2$, the electrode patterns and contact pads were written in 12 steps to obtain the higher electrode surface area.

## 2.2 Experimental Set-Up and Procedure

For the first experimental set-up we utilized PMMA 495K A2 not only as photoresist, but also as polarizable dielectric layer to produce charge patterns. The dielectric layer polarization is explained in details in section 1.3. 100 nm of aforementioned PMMA was spun on the electrode surface and the bonding pads were scratched and cleaned with acetone to provide electrical contact. Aluminum wires (d~0.5mm) were attached by using conductive paste to provide electrical contact. A second electrode coated with plain gold was used as counter electrode. It was placed on top of the dielectric layer to generate electric field and thus polarize PMMA sandwiched between two electrodes. Considering the fact that the electrode underneath the dielectric film has patterns and the gaps are insulators, polarization occurs only on the conductive area. Thus, the charge patterns on the surface replicate the electrode geometry shapes. DC power supply (RXN-302D-II) was used to apply potential across the electrodes. Negative polarity was given to

the top electrode with respect to the bottom electrode to obtain positive charge patterns on the surface.

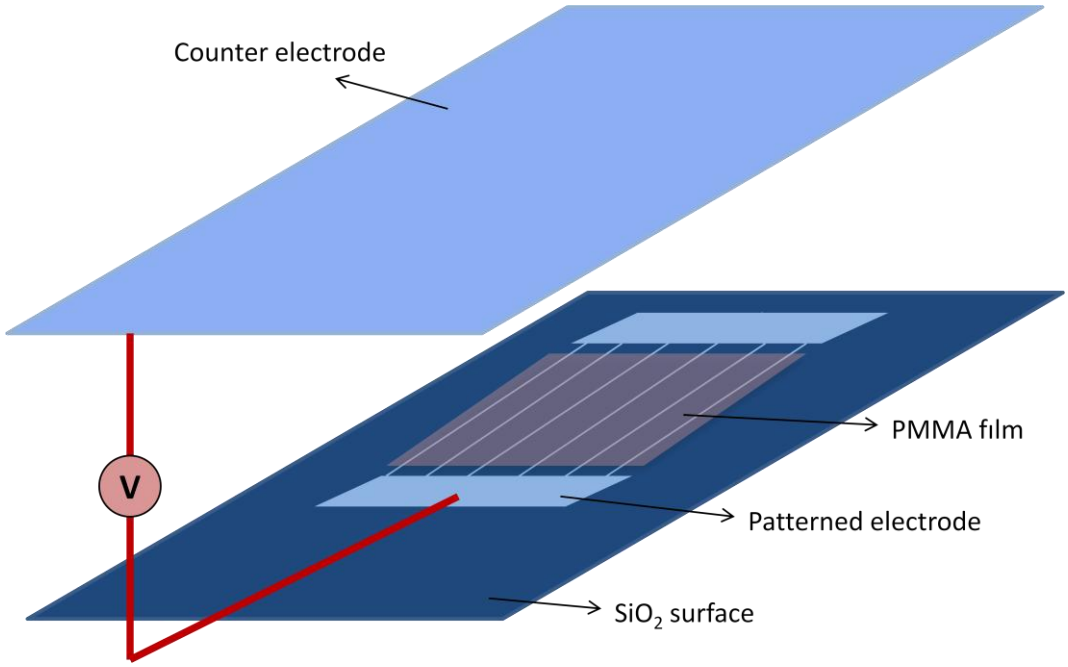


Figure 2. 8. Simple schematic view of the set-up for PMMA polarization

As a next step of the experimental procedure, we followed the protocol demonstrated by Palleau et. al [26]. After obtaining charge patterns, a droplet of desired aqueous dispersion was placed to the dielectric surface for a certain amount of time and it is followed by soaking the sample in a solvent with lower polarity than water to get rid of unwanted residues of the solvent. At last, the sample is dried by gently blowing nitrogen gas on to it and the aimed pattern is obtained. The process is shown in Figure 2.9.

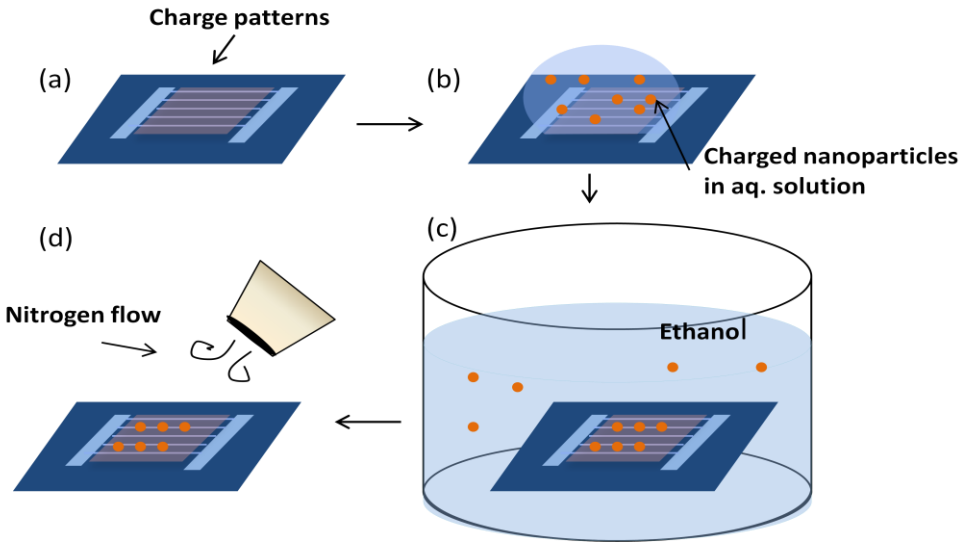


Figure 2.9. Schematics of the experimental procedure: (a) substrate with charge patterns; (b) dropping the nanoparticle solution to the surface for certain amount of time; (c) developing in ethanol to remove nanoparticles from undesired areas; (d) drying the surface.

The second experimental set-up incorporates the electrophoretic deposition (EPD) method. It also incorporates one working patterned electrode, a counter electrode a potentiostat. Two electrodes face each other and vertically immersed into the nanoparticle solution and voltage is applied across them for a certain amount of time. The electric field is generated in the solution between the electrodes and nanoparticles with known amount of surface charge are driven towards the oppositely charged electrode. As it was remarked in section 1.4, electrolysis occurring at the cathode and anode disturbs the particle assembly in aqueous solution. Therefore, pulsed DC voltage was applied instead continuous voltage to prevent this electrolysis [38]. Pulsed DC voltage was generated from wave function generator with 50% duty cycle pulse and monitored in oscilloscope and the signal was enhanced with the help of amplifier. Schematics of the electrophoretic deposition procedure performed in the experiments is shown in Figure 2.10

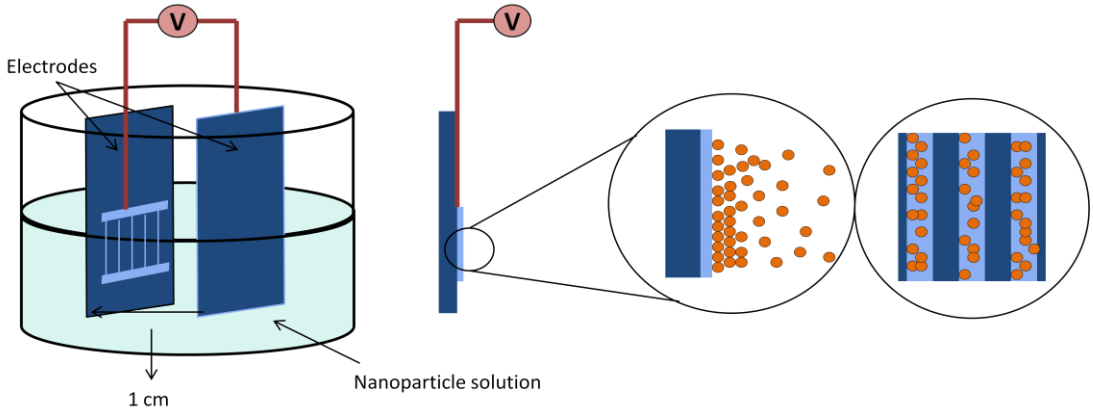


Figure 2.10. Schematics of experimental apparatus and nanoparticle assembly on the patterned electrode.

### 2.3 Nanoparticle Characterization

The test substances used in this study are colloidal gold and silver nanoparticles and fluorescent latex and silica nanoparticles. These particles are all spherical and in aqueous solutions and have positive or negative surface charge due to the capping agents. Only silver particles were synthesized in the laboratory [42] and all other solutions were purchased from Sigma Aldrich and hence they show high stability and monodispersity. Zeta (ζ) potentials were measured with Malvern Zetasizer Nano instrument. Parameters of nanoparticles used in the experiments are given in Table 2.2

Table 2.2. List of nanoparticles, their size, ζ-potentials and capping agents

| Nanoparticle | Diameter (nm) | ζ - potential (mV) | Capping Agent |
|---|---|---|---|
| Gold | 20 | -26.9±8 | Citrate(-$C_6H_5O_7$) |
| Silver | 80-100 | +61.8±11 | Polyethyleneimine(PEI) |
| Latex | 30 | -71.8±9 | Carboxylate (-COOH) |
| Silica | 30 | -24.8±9 | Amine (-$NH_2$) |

In addition, latex particles are fluorescent green (470/505nm) and silica particles are fluorescent red (569/585nm) which make them available to spot under the Fluorescent Microscope.

# Chapter 3

# RESULTS AND DISCUSSION

### 3.1 Directed Assembly of One Type of Nanoparticles

At the first stage of the experiments, it was aimed to control the assembly of one type of charged nanoparticles. For the set-up shown in Figure 2.8, voltages range from 5 to 30 V was applied and we concluded that 20 V is the optimum voltage. Voltage less than 20 V was not enough to polarize the PMMA and no nanoparticles patterns were observed. When more than 30 V of potential was applied, PMMA started to heat up due to the large amount of current transfer. Negative potential bias was sent to the electrode on top with respect to the bottom to attract positive charges on dielectric surface and hence to obtain positive charge patterns 30 µl of negatively charged colloidal gold dispersion was dropped to the polarized surface for 1 min followed by immersing the substrate to 10 ml of ethanol solvent for 1 min. After drying with $N_2$ flow, the surface was characterized under SEM.

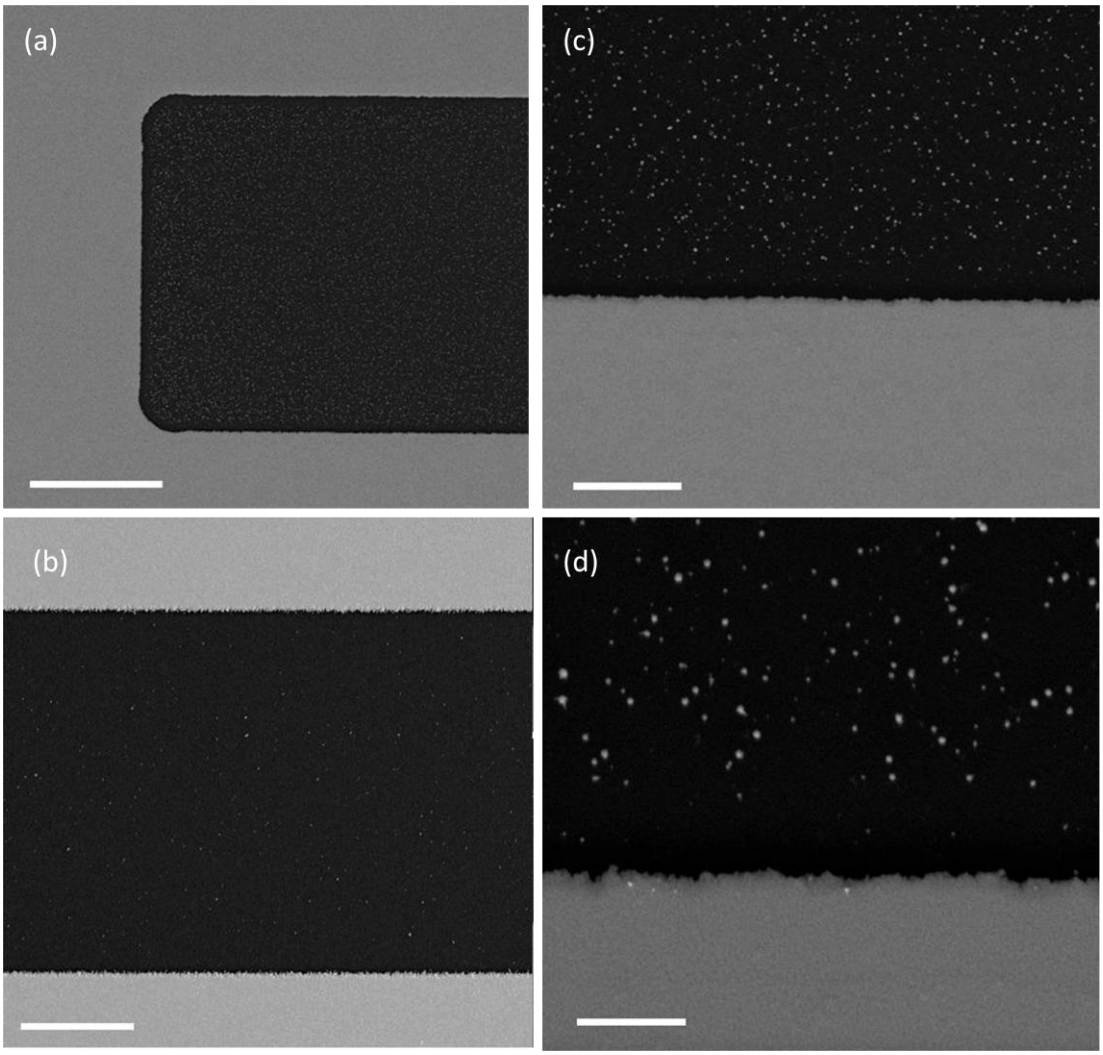


Figure 3.1. SEM micrographs of gold nanoparticles located in the gaps between the electrodes on the PMMA surface. Scale bars are 20, 15, 5 and 2μm for (a), (b). (c), (d) respectively.

As it is clear from the images, nanoparticles assemble in the gaps between the electrodes not on the electrodes as it was expected. The reason for that is the fringing fields emerging on the edges of the electrodes in which electric field is bended on the edges [43]. This creates the stronger attractions forces in the gaps which enables the particles to accumulate on those areas. The same procedure was applied for silver, latex and silica nanoparticles, however the results were not as successful as for the gold. Silver particles size is larger than the gold (~100nm) which means it requires higher amount of electrostatic forces to overcome the thermal diffusion of nanoparticles itself. As it was mentioned earlier, voltage limit is 30 V for 100 nm film PMMA polarization and it was not enough to direct

silver particles in controlled manner. For the case of latex and silica, they tend to agglomerate when the sample with the nanoparticle droplet is immersed into nonpolar solvent (ethanol in our case). That might be due to the high surface tension of latex and silica particles compared to the surface tension of the solvent. As a result, we constructed another experimental set-up which was shown in Figure 2.10 which is widely applied in deposition and coating research fields. Dielectric layer was removed and it allowed to increase the electrostatic attractive forces between patterned bare electrodes and charged nanoparticles. The assemblies of silver nanoparticles on the gold electrode surface can be seen in Figure 3.2 The applied voltage was 20 V across the electrodes for 5 mins and negative bias was applied to the electrode with the tori-shape pattern.

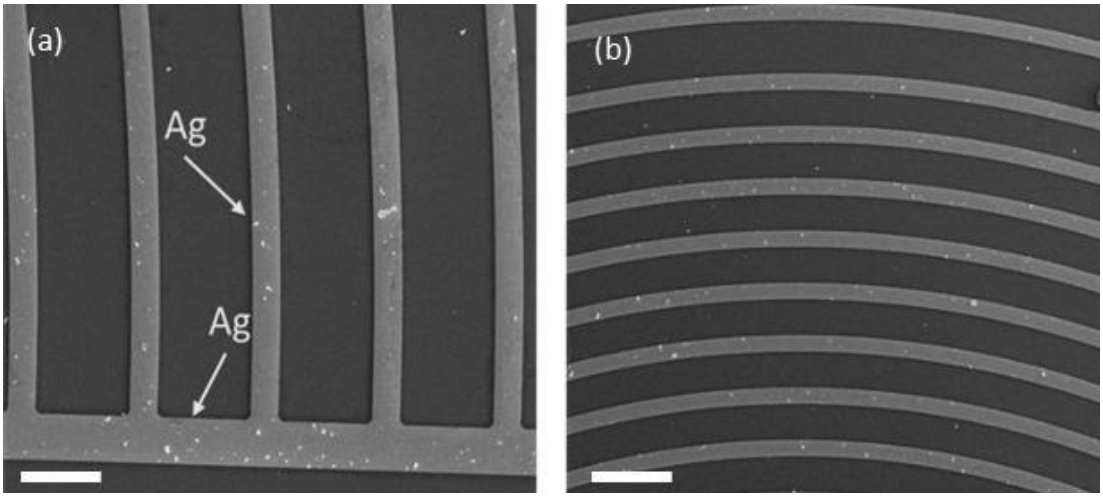


Figure 3.2. Silver nanoparticles accumulations on the tori-shape electrodes. Scale bars are 50 µ for (a) and 100 µm for (b).

When the deposition time was increased to 10 mins, there was no big difference on the assembled amount of particles since the density of the colloidal solution was low. As it was stated earlier, the one of the factors affecting the diffusion of particles is their size and density. Silver has both large diameter and density compared to latex and silica, and hence it's deposition is slower under the same experimental conditions. At voltages lower than 20 V, only few amount of deposited particles were observed.

Latex and silica nanoparticles were chosen as test objects since their fluorescent green and red colors respectively allows to differentiate between each other and

from other particles. Fluorescent micrographs of patterns of latex on the tori-shape electrode surface are shown in Figure 3.3. Besides few aggregations on some areas, the selective deposition was successful. It should be emphasized that the ζ-potential of latex particles is significantly high (~-70V) and therefore attractive forces with the charged electrode surface is stronger. 15 V of potential for 5 mins was enough for the diffusion and assembly of particles.

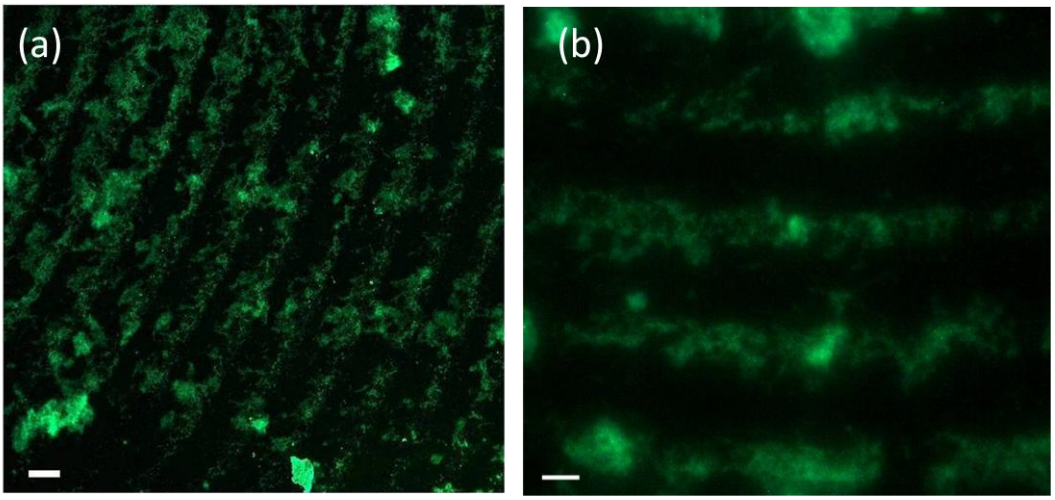


Figure 3.3. Fluorescent micrographs of latex nanoparticle assemblies on the tori-like electrode surface. Scale bars are 40 and 20 μm for (a) and (b) respectively.

The surface area of the electrodes fabricated with EBL is considerably smaller than surface area of the electrodes obtained from photolithography (800$\mu m^2$ vs. 8 mm for comb-like line electrode geometries). It directly affects the electric field strength generated between the electrodes and the nanoparticle migration. The voltage in this case was increased to 20V and the distance between the working and counter electrodes was decreased to 5 mm. As Figure 3.4 demonstrates, agglomeration of latex on the surface is lower compared to the one on bigger electrodes and the particles were directed to the desired areas on the surface.

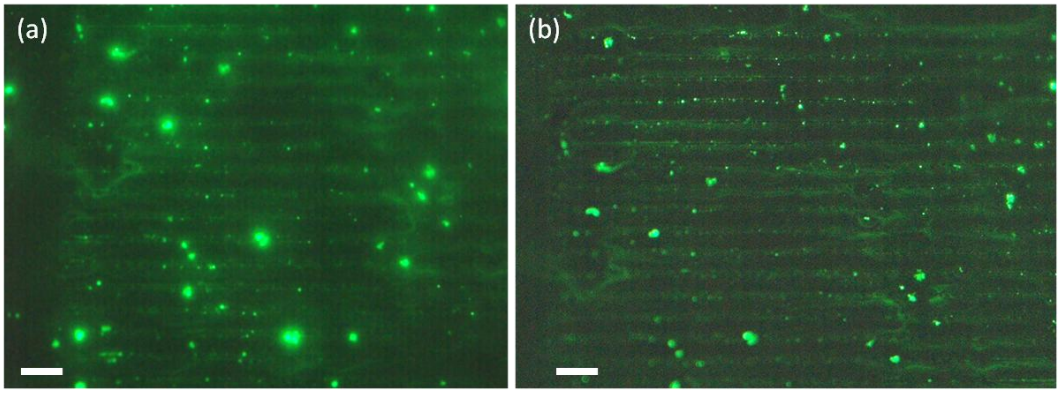


Figure 3.4. Latex nanoparticle patterns on 500 nm wide electrodes. Scale bar is 2µm for both images.

Subsequently, the directed assembly of one type of nanoparticles was once more confirmed with patterns of silica nanoparticles. The experimental parameters were the same as for latex particles. However, silica particles do not form aggregations on electrode surface due to its lower ζ-potential (~-24 mV). It can be noticed from Figure 3.5 that the particles tend to locate first to the edges of the electrodes first and then to the other sites. This the effect of fringing fields on the edges which generates the higher potential on those areas compared to the central parts. But fringing field effect is not as dominant as it was in the case of polarized dielectric surface.

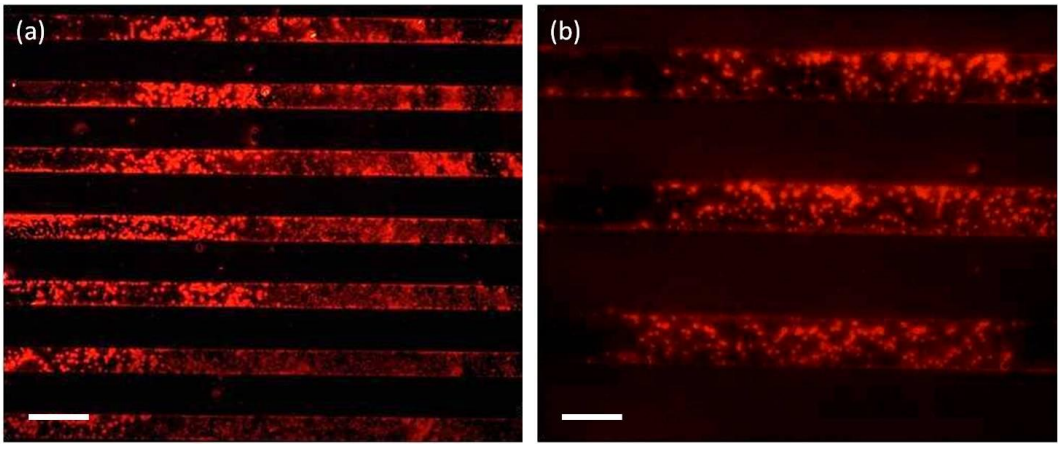


Figure 3.5. Fluorescent micrographs of silica nanoparticle patterns on rectangular electrodes. Scale bars indicate 50 and 20 µm for (a) and (b) respectively.

The distance between the electrodes obtained from EBL represented in Figure 3.6 is small compared to the other electrode designs from the same technique. Nevertheless, silica nanoparticles were selectively located on the metallic surfaces even if it is not perfectly uniform. Latex particles agglomerated and coated the whole electrode area on the similar structure.

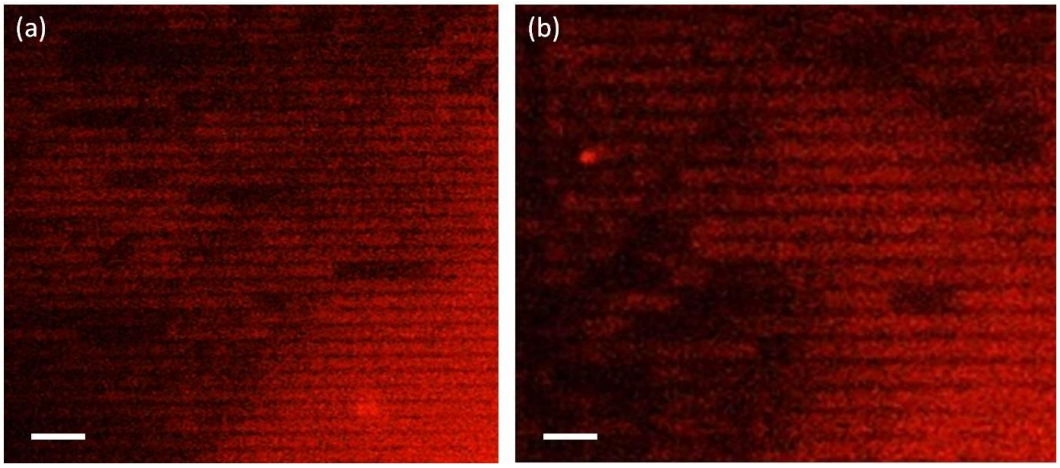


Figure 3.6. Silica nanoparticle deposition on 1 µm electrode lines. Scale bars are 4 and 2 µm for (a) and (b) respectively.

## 3.2 Directed Assembly of Two Types of Nanoparticles

### 3.2.1 Assembly of Nanoparticles on Different Sites of The Same Surface

The next stage of the study incorporates achieving the surfaces different types of nanoparticles on different locations of the same surface. The experimental set-up and working mechanism is the same as it was described earlier. In order to be able to apply two different types of voltages, comb-like electrode structures were used in the experiments. The shapes of these electrode geometries are shown in the fabrication section of the thesis. The electrode lines from two sides are positioned interchangeably. First, wire was connected to one side of the electrode and 15 V positive potential bias was applied with respect to the counter electrode. This leaves every other electrode on the line patterns neutral. The electrodes were immersed onto the latex nanoparticle solution for 5 mins and the substrate with patterns was disattached from wire and was dried under $N_2$ blow. Figure 3.7a

confirms that latex nanoparticles skip every second electrode and are positioned only on the areas which were biased with positive potential. After the characterization, the other side of the electrode on the same was now connected to wire and positive potential was applied while immersing the electrodes into the silica nanoparticle solution. It should be expected that silica particles should migrate only to the electrode areas which are

charged and skip the sites which are already coated with latex. Nonetheless, it is evident from Figure 3.7b that some amount of particles is nonselectively grafted on the neighboring electrodes as well. The density of the particles assembled on the charged surfaces is yet higher. The surfactant of latex particles is carboxilate groups and they are anionic as it was confirmed with ζ-potential results. On the other hand, the amine capping agent in silica solution is zwitterionic. It means, it can carry both positive and negative surface charge depending on the environment. The net surface potential of silica is negative however it also carries some amount of positive potential. Since latex particles which are already assembled on the electrodes are highly negatively charged, positive charge induced from amine molecules in silica might be attracted towards the latex as well.

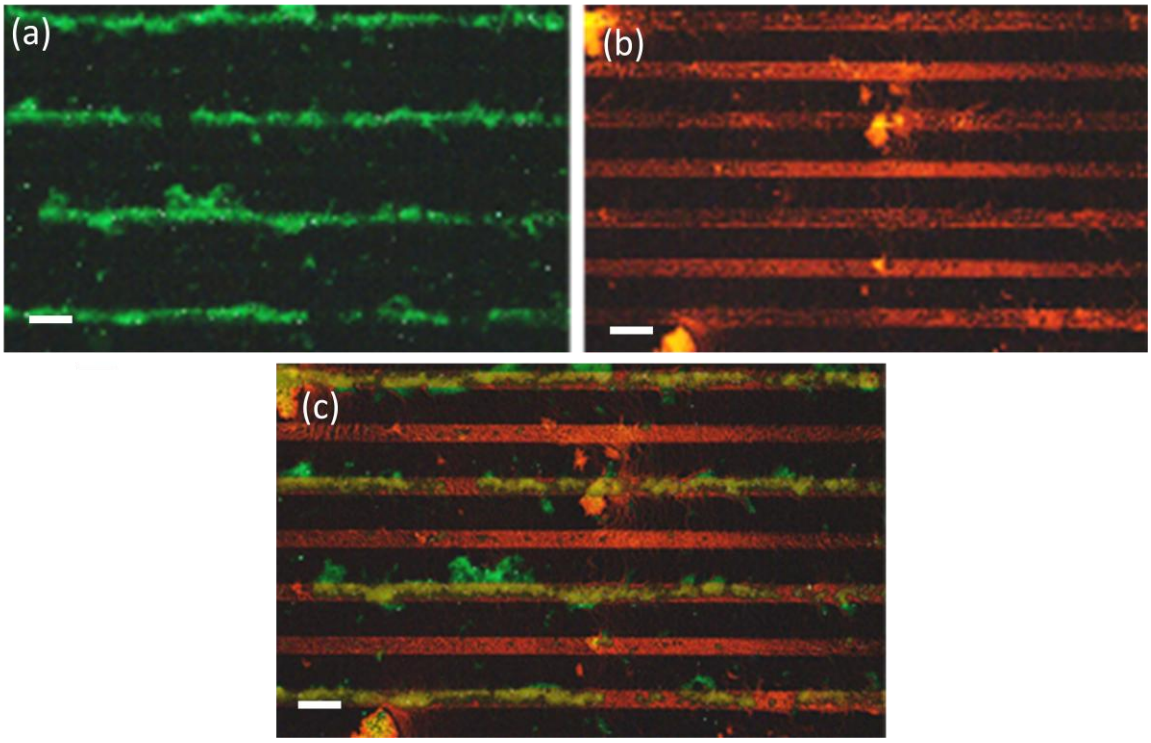


Figure 3. 7. Assemblies of latex (a) and silica (b) nanoparticles positioned next to each other; (c) superpositioned image of (a) and (b) to demonstrate the two types of particles are on the same surface. Scale bar 20 μm for all images.

The results can be considered as successful but the improvements can be done in the future by using different nanoparticles which is capped in only anionic or cationic surfactant.

### 3.2.2 Assembly of Nanoparticles on The Same Sites of The Surface

The last stage of this work describes the procedure of obtaining composite surfaces by attracting two types of nanoparticles to the same locations of the surface. The experimental process is similar to the one explained in previous section. The only difference is that instead comb-like electrodes, regular arrays of electrodes was used and hence the potential was applied to the same metallic surfaces twice. Briefly, electrodes were immersed into silica nanoparticle solution while 15 V of positive voltage was applied to the patterned electrode followed by changing the solution into the one containing latex particles after 5 mins without interrupting the voltage bias. After the deposition of latex for 5 mins as well, the sample was dried and composite structures were obtained successfully. Figure

3.8a and 3.8b confirms that both silica and latex are on the same electrode surfaces. Since silica can be viewed under suitable light for red fluorescence and latex can be seen under the light for green fluorescence at the same time, it can be concluded that the electrode surface is coated with the mixture of the both nanoparticles and latex is not completely on top of silica. Since the fluorescent microscope that is used for our project cannot display both red and green colors at the same time, two images taken from the same area were put on top of each other to show the composite structure patterns more clearly.

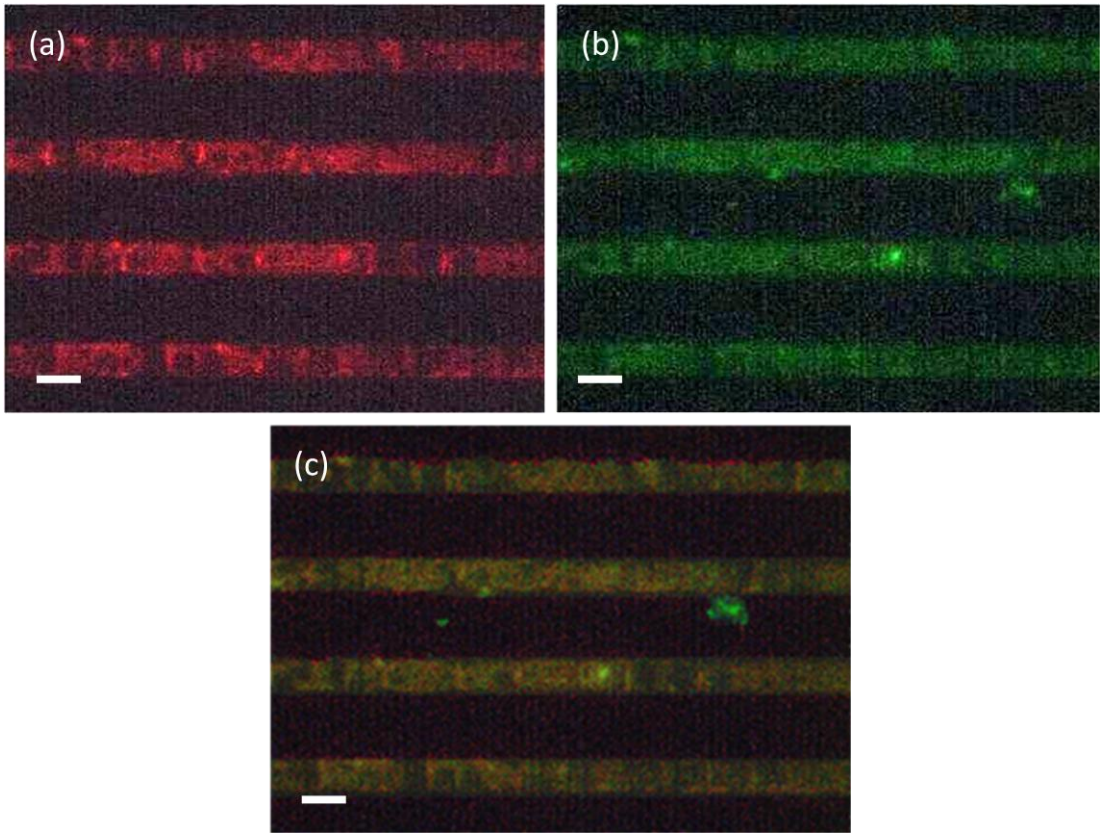


Figure 3. 8. Composite patterns containing silica (a) and latex (b) assembled on 20 µm wide electrodes ; (c) combination of (a) and (b) to show that both particles are on the same surface. Scale bar is 20 µm for all images.

When the particles are deposited on the smaller electrode surface and when the distance between the electrodes are not that large, latex particles tend to aggregate on some areas and the density of the particles are higher on some other areas. But

it general, latex follows the electrode geometry (Figure 3.9a). The deposition of silica is more uniform and the pattern can be observed clearly (Figure 3.9b)

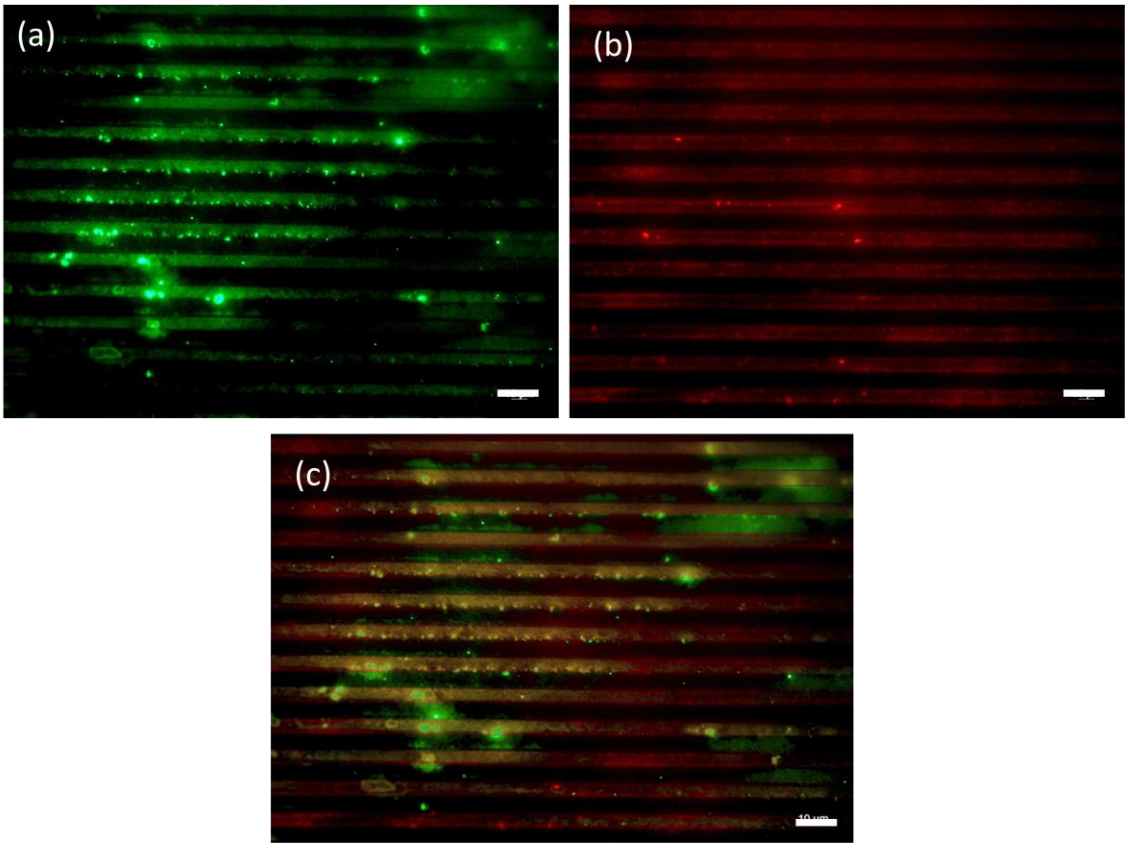


Figure 3.9. Composite patterns containing silica (a) and latex (b) assembled on 5 µm wide electrodes ; (c) combination of (a) and (b) to show that both particles are on the same surface. Scale bar is 10 µm for all images.

It should be noted that all nanoparticles used in this study were in aqueous solutions and therefore pulsed DC voltage (instead of continuous DC) was applied across the electrodes for all the experiments. Little amount of bubbling was observed on the edges of the electrodes however it is negligible and did not interrupt the particle diffusion. Nonpolar solvents are favorable to avoid electrolysis when regular DC voltage is applied (as it worked for silver nanoparticle dispersed in ethanol) however latex and silica became unstable immediately after adding few droplets of ethanol to the solutions.

# Chapter 4

# CONCLUSION AND FUTURE OUTLOOK

In summary, the patterns of different types of nanoparticles were obtained on both dielectric and metallic surfaces by causing the electrostatic forces between the electrodes and the charged particles. Electrodes were fabricated from photolithography and electron beam lithography for a better resolution.

At the first stage of the study, assemblies of one type of particles were generated on the surface. Aqueous dispersions of gold, silver, fluorescent latex and silica were utilized for experimental tests. The results indicate that more precise and finer depositions can be produced on structured metallic surfaces when the large amount of electric field is applied. On the other hand, it was observed that as ζ-potential of the solution is higher, particles got deposited faster and more uniformly.

At the second stage, the binary assemblies of latex and silica particles were produced on the desired locations of the surface. First, latex was patterned on one electrode structure followed by patterning silica on the other electrode on the same surface. Due to the comb-like shape of the electrodes, patterns of latex and silica alter on each electrode line. Since the silica surfactant is zwitterionic, some amount of silica was observed on latex patterns and hence the results can be improved by simply changing the nanoparticle dispersant.

At last, structured composite surfaces were created from silica and latex particles. The patterns of these composited were controlled by the electrode shape.

The method that is used here is applicable for any kind of conductive electrode surface and any kind of charged nanomaterial in fluidic medium. The patterns of any shape can be produced and the resolution is dependent on electrode dimensions. This flexibility opens up possibilities for designing devices with a desired pattern and nanoparticle composition. The results are promising for developing multifunctional and highly efficient nanosensors. For example, a gas sensor composed of independent patterns of two types of nanoparticles (e.g. Au and $Fe_3O_4$) will have capability of detecting two types of gases in air. Moreover, the ability to manipulate materials makes it possible to deposit the mixture of biological materials on different locations of the same surface for their further study and analysis separately.

For further improvements of the results, the distribution of particles on the surface will be studied quantitatively. The adhesion strength of particles on to the electrodes will be examined and analyzed in different environments (e.g. high temperature, in fluidic medium), since it's a crucial factor for the versatility of the applications of these patterned surfaces.

# BIBLIOGRAPHY


[1] C. B. Murray, D.J. Norris and M.G. Bawendi, "Synthesis and Characterization of Nearly Monodisperse CdE (E = Sulfur, Selenium, Tellurium) Semiconductor Nanocrystallites." *Journal of the American Chemical Society*, vol. 115, no. 19, pp. 8706–8715, 1993.

[2] I. L. Medinz, H. T. Uyeda, E. R. Goldman and H. Mattoussi, "Quantum Dot Bioconjugates for Imaging, Labelling and Sensing." *Nature Materials*, vol. 4, no. 6, pp. 435–446, 2005.

[3] M. Zorn, W. K. Bae, J. Kwak, H. Lee, C. Lee, R. Zentel and K. Char, "Quantum Dot−Block Copolymer Hybrids with Improved Properties and Their Application to Quantum Dot Light-Emitting Devices." *ACS Nano*, vol. 3, no. 5, pp. 1063–1068, 2009.

[4] Y. Choi, M. Seol, W. Kim and K. Yong "Chemical Bath Deposition of Stoichiometric CdSe Quantum Dots for Efficient Quantum-Dot-Sensitized Solar Cell Application." *The Journal of Physical Chemistry C*, vol. 118, no. 11, pp. 5664–5670, 2014.

[5] N. S. Beattie, P. See, G. Zoppi, P. M. Ushasree, M. Duchamp, I. Farrer, D. A. Ritchie and S. Tomic "Quantum Engineering of InAs/GaAs Quantum Dot Based Intermediate Band Solar Cells." *ACS Photonics*, vol. 4, no. 11, pp. 2745–2750, 2017.

[6] N. Morgan, C. Leatherdale, M. Drnic, M. Jarosz, M. Kastner and M. Bawendy "Electronic Transport in Films of Colloidal CdSe Nanocrystals." *Physical Review B*, vol. 66, no. 7, pp. 1-9, 2002.

[7] W. Song, H. Li, W. Qiang and D. Xu "Disposable Electrochemical Aptasensor Array by Using in Situ DNA Hybridization Inducing Silver Nanoparticles Aggregate for Signal Amplification." *Analytical Chemistry*, vol. 86, no. 5, pp. 2775–2783, 2014.

[8] A. J. Coughlin and J. L. West. "Targeting Gold Nanoparticles for Cancer Diagnostics and Therapeutics." *ACS Symposium Series Functional Nanoparticles for Bioanalysis, Nanomedicine, and Bioelectronic Devices Volume 2*, pp. 37–54, 2012.

[9] W. Eck, A. I. Nicholson, H. Zentgraf, W. Semmerland and S. Bartling, "Anti-CD4-Targeted Gold Nanoparticles Induce Specific Contrast Enhancement of Peripheral Lymph Nodes in X-Ray Computed Tomography of Live Mice." *Nano Letters*, vol. 10, no. 7, pp. 2318–2322, 2010.

[10] Q. Pankhurst, S. Jones and J. Dobson, "Applications of Magnetic Nanoparticles in Biomedicine: the Story so Far." *Journal of Physics D: Applied Physics*, vol. 49, no. 50, p. 501002, 2016.

[11] A. C. Hunter, J. Elsom, P.P Wibroe, S. M. Moghimi, "Polymeric Particulate Technologies for Oral Drug Delivery and Targeting: A Pathophysiological Perspective." *Maturitas*, vol. 73, no. 1, pp. 5–18, 2012.

[12] H. Goesmann and C. Feldmann. "ChemInform Abstract: Nanoparticulate Functional Materials." *ChemInform*, vol. 41, no. 20, pp. 1362-1395, 2010.

[13] Terris, B D, and T Thomson. "Nanofabricated and Self-Assembled Magnetic Structures as Data Storage Media." *Journal of Physics D: Applied Physics*, vol. 38, no. 12, pp. 199-222 2005.

[14] Krauss and P. J. Renstrom, "Imprint Lithography with 25-Nanometer Resolution." *Science*, vol. 272, no. 5258, pp. 85–87, 1996.

[15] J. W. Jeong, W. I Park, L. M. Do, J. H. Park, T. H. Kim, G. Chae and Y. S. Jung "Nanotransfer Printing with Sub-10 Nm Resolution Realized Using

Directed Self-Assembly." *Advanced Materials*, vol. 24, no. 26, pp. 3526–3531, 2012.

[16] Y. S. Jung, W. Jung, H. L. Tuller and C. A. Ross "Nanowire Conductive Polymer Gas Sensor Patterned Using Self-Assembled Block Copolymer Lithography." *Nano Letters*, vol. 8, no. 11, pp. 3776–3780, 2008.

[17] I. Park, S. H. Ko, H. Pan, C. P. Grigoropoulos, A. P. Pisano, J. M. J. Frechet, E. S. Lee and J. H. Jeong "Nanoscale Patterning and Electronics on Flexible Substrate by Direct Nanoimprinting of Metallic Nanoparticles." *Advanced Materials*, vol. 20, no. 3, pp. 489–496, 2008.

[18] M. T. Demko, J. C. Cheng and A. P. Pisano "High-Resolution Direct Patterning of Gold Nanoparticles by the Microfluidic Molding Process." *Langmuir*, vol. 26, no. 22, pp. 16710–16714, 2010.

[19] H. Sirringhaus, T. Kawase, R. H. Friend, T. Shimoda, M. Inbasekaran, W. Wu and E. P. Woo "High-Resolution Inkjet Printing of All-Polymer Transistor Circuits." *Science*, vol. 290, no. 5499, pp. 2123–2126, 2000.

[20] S, H. Ko, J. Chung, H. Pan, P. Grigopoulos and D. Poulikakos "Fabrication of Multilayer Passive and Active Electric Components on Polymer Using Inkjet Printing and Low Temperature Laser Processing." *Sensors and Actuators A: Physical*, vol. 134, no. 1, pp. 161–168, 2007.

[21] N. R. Wood, A. I. Wolsiefer, R. W. Cohn and S. J. Williams "Dielectrophoretic Trapping of Nanoparticles with an Electrokinetic Nanoprobe." *Electrophoresis*, vol. 34, no. 13, pp. 1922-1933, 2013.

[22] H. O. Jacobs, S. A. Campbell and M. G. Steward "Approaching Nanoxerography: The Use of Electrostatic Forces to Position Nanoparticles with 100 Nm Scale Resolution." *Advanced Materials*, vol. 14, no. 21, pp. 1553–1557, 2002.

[23] C. R. Barry,M. G. Steward, N. Z. Lwin and H. O. Jacobs “Printing Nanoparticles from the Liquid and Gas Phases Using Nanoxerography.” *Nanotechnology*, vol. 14, no. 10, pp. 1057–1063, 2003.

[24] C, R, Barry, J. Gu, H. O. Jacobs “Charging Process and Coulomb-Force-Directed Printing of Nanoparticles with Sub-100-Nm Lateral Resolution.” *Nano Letters*, vol. 5, no. 10, pp. 2078–2084, 2005.

[25] M. Kolíbal, M. Konecny, F. Ligmajer, D. Skoda, T. Vystavel, J. Zlamal, P. Varga and T. Sikola “Guided Assembly of Gold Colloidal Nanoparticles on Silicon Substrates Prepatterned by Charged Particle Beams.” *ACS Nano*, vol. 6, no. 11, pp. 10098–10106, 2012.

[26] P. Moutet, L. M. Lacroix, A. Robert, M. Imperor-Clerc, G. Viau and L. Ressier “Directed Assembly of Single Colloidal Gold Nanowires by AFM Nanoxerography.” *Langmuir*, vol. 31, no. 14, pp. 4106–4112, 2015.

[27] E. Palleau, N. M. Sangeetha, G. Viau, J. D. Marty and L. Ressier “Coulomb Force Directed Single and Binary Assembly of Nanoparticles from Aqueous Dispersions by AFM Nanoxerography.” *ACS Nano*, vol. 5, no. 5, pp. 4228–4235, 2011.

[28] E. Palleau, L. Ressier, L. Borowik and T. Melin “Numerical Simulations for a Quantitative Analysis of AFM Electrostatic Nanopatterning on PMMA by Kelvin Force Microscopy.” *Nanotechnology*, vol. 21, no. 22, pp. 225706-225382, 2010.

[29] D. Morales, L. Teulon, E. Palleau, T. Alnasser and L. Ressier, “Single-Step Binary Electrostatic Directed Assembly of Active Nanogels for Smart Concentration-Dependent Encryption.” *Langmuir*, vol. 34, no. 4, pp. 1557–1563, 2018.

[30] Y. G. Guo, J. S. Hu, H. P. Liang, L. J. Wan and C. L. Bai, “TiO2-Based Composite Nanotube Arrays Prepared via Layer-by-Layer Assembly.” *Advanced Functional Materials*, vol. 15, no. 2, pp. 196–202, 2005.

[31] B. Yu, K. M. Leung, Q. Guo, W. M. Lau and J. Yang, “Synthesis of Ag–TiO2composite Nano Thin Film for Antimicrobial Application.” *Nanotechnology*, vol. 22, no. 11, pp. 115603-115611, 2011.

[32] J. Borges and J. F. Mano, “Molecular Interactions Driving the Layer-by-Layer Assembly of Multilayers.” *Chemical Reviews*, vol. 114, no. 18, pp. 8883–8942, 2014.

[33] H. Ohshima and K. Makino, “Colloid and Interface Science in Pharmaceutical Research and Development ”, Elsevier, p. 3, 2014.

[34] D. J. Shaw, “Colloid & Surface Chemistry”, *Butterworth Heinemann*, San Francisco, pp. 174-189, 2000.

[35] F. Li, D. P. Josephson and Stein, “Colloidal Assembly: The Road fromParticles to Colloidal Molecules and Crystals*.” Angew. Chem. Int. Ed.*, vol. 50, no.12, pp. 360-388, 2010.

[36] J. Orrit-Prat, L. Boudou, C. Villeneuve, G. Teyssedre, S. Behar, L. Ressier and R. Diaz, “Effect of Film Thickness on the Dielectric Properties and Charge Storage in PMMA Thin Films.” *2013 IEEE International Conference on Solid Dielectrics (ICSD)*, 2013.

[37] P. Sarkar and P. S. Nicholson, “Electrophoretic Deposition (EPD): Mechanisms, Kinetics, and Application to Ceramics.” *Journal of the American Ceramic Society*, vol. 79, no. 8, pp. 1987–2002, 1996.

[38] W. Guo and B. Liu, “Liquid-Phase Pulsed Laser Ablation and Electrophoretic Deposition for Chalcopyrite Thin-Film Solar Cell Application.” *ACS Applied Materials & Interfaces*, vol. 4, no. 12, pp. 7036–7042, 2012.

[39] A. J. Krejci, I. Gonzalo-Juan and J. H. Dickerson, “Evolution of Ordering in Iron Oxide Nanoparticle Monolayers Using Electrophoretic Deposition.” *ACS Applied Materials & Interfaces*, vol. 3, no. 9, pp. 3611–3615, 2011.

[40] M. A. Islam, Y. Xia, D. A. Telesca, M. L. Steigerwald and I. P. Herman, "Controlled Electrophoretic Deposition of Smooth and Robust Films of CdSe Nanocrystals." *Chemistry of Materials*, vol. 16, no. 1, pp. 49–54, 2004.

[41] S. D. Oberdick and S. A. Majetich. "Electrophoretic Deposition of Iron Oxide Nanoparticles on Templates." *The Journal of Physical Chemistry C*, vol. 117, no. 36, pp. 18709–18718, 2013.

[42] L. Besra, T. Uchikoshi, T. S. Suzuki and Y. Sakka, "Application of Constant Current Pulse to Suppress Bubble Incorporation and Control Deposit Morphology during Aqueous Electrophoretic Deposition (EPD)." *Journal of the European Ceramic Society*, vol. 29, no. 10, pp. 1837–1845, 2009.

[43] M. Ammam, "Electrophoretic Deposition under Modulated Electric Fields: a Review." *RSC Advances*, vol. 2, no. 20, pp. 7633-7646, 2012.

[44] A. Sharonova, K. Loza, M. Surmeneva, O. Prmyak and M. Epplw "Synthesis of Positively and Negatively Charged Silver Nanoparticles and Their Deposition on the Surface of Titanium." *IOP Conference Series: Materials Science and Engineering*, vol. 116, 2016.

[45] C. R.Barry and Heiko O. Jacobs. "Fringing Field Directed Assembly of Nanomaterials." *Nano Letters*, vol. 6, no. 12, pp. 2790–2796, 2006.

# APPENDIX A

## Synthesis of Positively Charged Silver Nanoparticles

Silver nitrate ($AgNO_3$) salt, a stabilizer Polyethylenimine (PEI) branched average Mw ~25,000 were purchased from Sigma-Aldrich. Double deionized (DDI) water was obtained from Millipore/Direct Q-3UV water purification system. Sharonova's method was used to obtain the positively charged silver nanoparticle (Ag-NPs) [40]. The reaction medium was prepared by dissolving 2.5 wt% PEI in 10ml DDI water. The reaction medium was magnetically stirred at 250 rpm and heated up to $90^0$C in oil bath. The silver precursor was prepared as 0.125g $AgNO_3$ was dissolved in 250 µl DDI. This precursor solution was added into reaction medium. The dispersion medium was mixed at $90^0$C for 1 hour. The color of the dispersion medium was changed from yellowish to metallic black or dark gray color. The positively charged Ag-NPs were collected from medium by 15000rpm centrifugation for 15min. The black precipitate was washed by DDI water. The positively charged Ag-NPs were kept at room temperature in DDI water or absolute ethanol for further studies.

ζ-potential measurements show that the suspension is stable and surface potential is +62±9.64 mV (Figure A1.)

| | | Mean (mV) | Area (%) | Width (mV) |
|---|---|---|---|---|
| Zeta Potential (mV): 62.0 | Peak 1: | 62.0 | 100.0 | 9.64 |
| Zeta Deviation (mV): 9.64 | Peak 2: | 0.00 | 0.0 | 0.00 |
| Conductivity (mS/cm): 0.0140 | Peak 3: | 0.00 | 0.0 | 0.00 |

**Result quality** Good

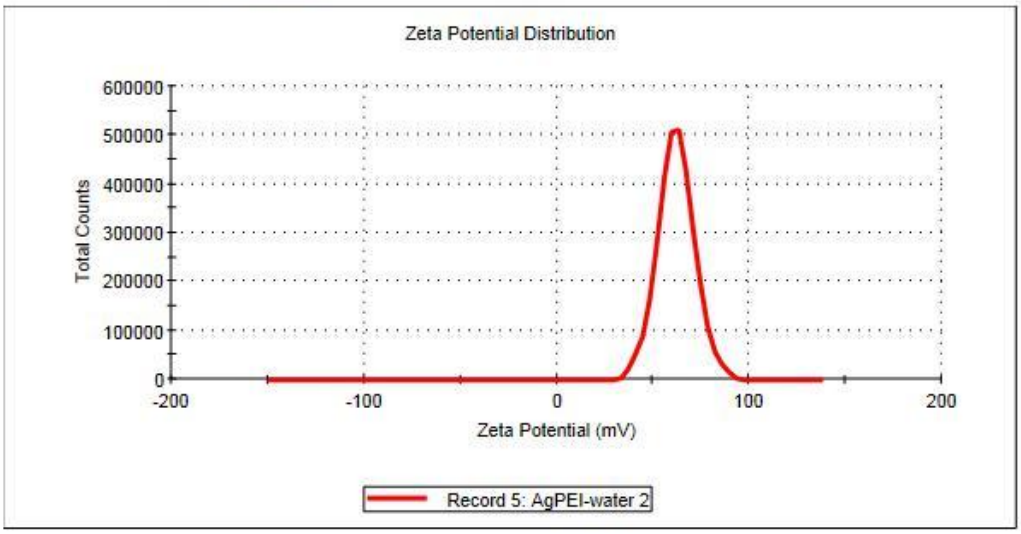


Figure A1. Zeta potential curve for positively charged silver nanoparticles.